The L-isoaspartate modification within protein fragments in the aging lens can promote protein aggregation

Rebeccah A. Warmack[‡§1], Harrison Shawa[‡§], Kate Liu[‡§2], Katia Lopez[‡§], Joseph A. Loo[‡§3], Joseph Horwitz[§¶4], and Steven G. Clarke[‡§5]

From the ‡Department of Chemistry and Biochemistry, the §Molecular Biology Institute, and the ¶Jules Stein Eye Institute, UCLA, Los Angeles, California 90095

Edited by John M. Denu

Transparency in the lens is accomplished by the dense packing and short-range order interactions of the crystallin proteins in fiber cells lacking organelles. These features are accompanied by a lack of protein turnover, leaving lens proteins susceptible to a number of damaging modifications and aggregation. The loss of lens transparency is attributed in part to such aggregation during aging. Among the damaging post-translational modifications that accumulate in long-lived proteins, isomerization at aspartate residues has been shown to be extensive throughout the crystallins. In this study of the human lens, we localize the accumulation of L-isoaspartate within water-soluble protein extracts primarily to crystallin peptides in high-molecular weight aggregates and show with MS that these peptides are from a variety of crystallins. To investigate the consequences of aspartate isomerization, we investigated two αA crystallin peptides [52]LFRTVLDSGISEVR[65] and [89]VQDDFVEIH[98], identified within this study, with the L-isoaspartate modification introduced at Asp[58] and Asp[91], respectively. Importantly, whereas both peptides modestly increase protein precipitation, the native [52]LFRTVLDSGISEVR[65] peptide shows higher aggregation propensity. In contrast, the introduction of L-isoaspartate within a previously identified anti-chaperone peptide from water-insoluble aggregates, αA crystallin [66]SDRDKFVIFL(isoAsp)VKHF[80], results in enhanced amyloid formation *in vitro*. The modification of this peptide also increases aggregation of the lens chaperone αB crystallin. These findings may represent multiple pathways within the lens wherein the isomerization of aspartate residues in crystallin peptides differentially results in peptides associating with water-soluble or water-insoluble aggregates. Here the eye lens serves as a model for the cleavage and modification of long-lived proteins within other aging tissues.

The synthesis of the main structural proteins of the mammalian lens, the crystallins, begins during embryonic lens development within the primary fiber cells, which eventually comprise the lens core, termed the lens nucleus (1). Crystallin synthesis is followed by the loss of the cellular nucleus and other organelles via autophagy, mitophagy, and nucleophagy to minimize light scattering (2). The resulting fiber cells are largely devoid of protein turnover machinery yet contain protein concentrations upwards of 450 mg/ml in the human lens. These high protein concentrations provide lens transparency via short-range order interactions that minimize errors in refraction by destructive interference (3, 4). These proteins, many of which have been synthesized by the time of birth, are not protected by the same turnover mechanisms present in normal somatic cells and are thus susceptible to spontaneous, age-related covalent modifications and aggregation.

Post-translational modifications that accumulate over time have been identified within all of the major crystallin families: α, β, and γ. These alterations are largely age-dependent spontaneous reactions leading to deamidation, isomerization, racemization, oxidation, and glycation (5, 6). Among these, isomerization and deamidation have been extensively characterized in the aged lens (7–11). The primary mechanism of asparagine deamidation and aspartate isomerization involves the formation of an intermediate L-succinimide ring, which can be hydrolyzed at either of its two carbonyls, resulting in either L-Asp or L-isoaspartate (L-isoAsp;[6] Fig. 1). Additionally, the L-succinimide intermediate can racemize to D-succinimide and yield D-Asp or D-isoaspartate (D-isoAsp). The major products of these reactions are L-isoaspartyl residues (12). Deamidation can affect the structural integrity of proteins through the introduction of a negative charge, but L-isoAsp is particularly harmful at both asparagine and aspartate sites within proteins due to the

Figure 1. Pathway for L-isoAsp formation and repair. Normal L-asparagine and L-aspartate residues (*top*) can undergo deamidation or dehydration, respectively, to yield a five-membered L-succinimide ring (*center*), which is readily hydrolyzed under cellular conditions to yield either L-aspartate (~15–40% of product) or, more frequently, L-isoaspartate (~60–85%; *bottom left*) (15). This abnormal residue can be repaired by reactions initiated by the L-isoaspartyl/D-aspartyl O-methyltransferase PCMT1, which uses AdoMet as a methyl donor to create a methyl ester that can be quickly hydrolyzed back under cellular conditions to the L-succinimide intermediate, allowing the reformation of L-aspartate residues. The L-succinimide ring can racemize during this pathway and yield D-aspartate and D-isoaspartate isomers, which are not shown here. D-Aspartate is an additional substrate for the PCMT1 repair enzyme (albeit with k_{cat}/K_m values reduced 1000-fold or more (17), whereas D-isoaspartate is not a substrate. Adapted from Ref. 56. This research was originally published in Int. J. Pept. Protein Res. Clarke, S. Propensity for spontaneous succinimide formation from aspartyl and asparaginyl residues in cellular proteins. *International Journal of Peptide and Protein Research.* 1987; 30:808–821 . © John Wiley & Sons.

addition of a backbone methylene group that effectively "kinks" the polypeptide chain (13). Aspartate isomerization products can be difficult to distinguish from normal aspartyl residues with canonical MS techniques, and their identification remains challenging, often requiring specific fragmentation methods such as electron transfer dissociation, electron capture dissociation, or complex labeling strategies (14, 15). Because of these difficulties, our understanding of L-isoAsp modifications within the context of the human lens is still incomplete.

There is a repair pathway within most cells, including the lens fiber cells, that results in the conversion of L-isoaspartyl to L-aspartyl residues by the L-isoaspartate (D-aspartate) *O*-methyltransferase (PCMT1) (16, 17). The major PCMT1 activity initiates the recognition of L-isoaspartyl residues forming methyl esters that can then spontaneously result in their conversion to normal L-aspartate residues. This enzyme can also recognize D-aspartyl residues with a much lower affinity (at least 700 times) in reactions that can lead to eventual D-isoaspartyl formation (18). However, it has been shown that aspartate isomers are still present within lens proteins. Various groups have shown the accumulation of the four Asp isomers at specific sites, particularly within the α crystallins of aged and cataractous lenses (19–24). The accumulation of these residues presumably reflects the rate of their formation and the rate of their removal by either repair or degradation reactions. However, the effects of these modifications on lens function remain unclear. Takata and Fujii (25) linked aspartate isomerization to dissociation of crystallins from the native oligomeric form. Other studies have shown deamidation within crystallins *in vitro* to be associated with aggregation (6).

Here we investigated the localization, extent, and possible consequences of L-isoAsp accumulation within the human lens. We took advantage of the specificity of PCMT1 and the high sensitivity of radiolabeling techniques to demonstrate that L-isoAsp residues accumulate within the aged lens to high levels, with the greatest accumulation in the urea-solubilized water-insoluble (WI) nuclear extract proteins. Size-exclusion separation of water-soluble (WS) lens extracts followed by radiolabeling and SDS-PAGE separation of polypeptides containing L-isoaspartyl reveals that the highest levels of labeled residues are localized to aggregated low-molecular weight (LMW) protein fragments that migrate primarily below 14 kDa on SDS-PAGE. Mass spectrometry of these LMW species shows that these fragments come from a number of different lens proteins. Finally, to investigate the potential consequences of this modification within lens protein fragments, we probed the effects of L-isoAsp residues in αA crystallin–derived peptides. Our assays within three peptides revealed that the introduction of the L-isoAsp residue can increase or decrease the aggregation tendencies of the given peptide, which may dictate whether peptides in the lens eventually become primarily WI- or WS-associated.

Results

L-*Isoaspartyl residues accumulate to high levels within WS and urea-solubilized WI extracts of aged lenses despite endogenous PCMT1 activity*

Purified recombinant L-isoaspartyl/D-aspartyl protein methyltransferase PCMT1 was used as an analytical probe with [³H]AdoMet to specifically label L-isoAsp residues and to quantitate the extent of isomerization by detecting [³H]methanol in a volatility assay after base hydrolysis of the [³H]methyl esters formed in the incubation. L-isoAsp content in the WS and urea-solubilized WI extracts of whole human lenses from ages spanning 26–76 years old was observed to increase with age (Fig. 2A). Levels for the WI extracts were ~5-fold higher than the
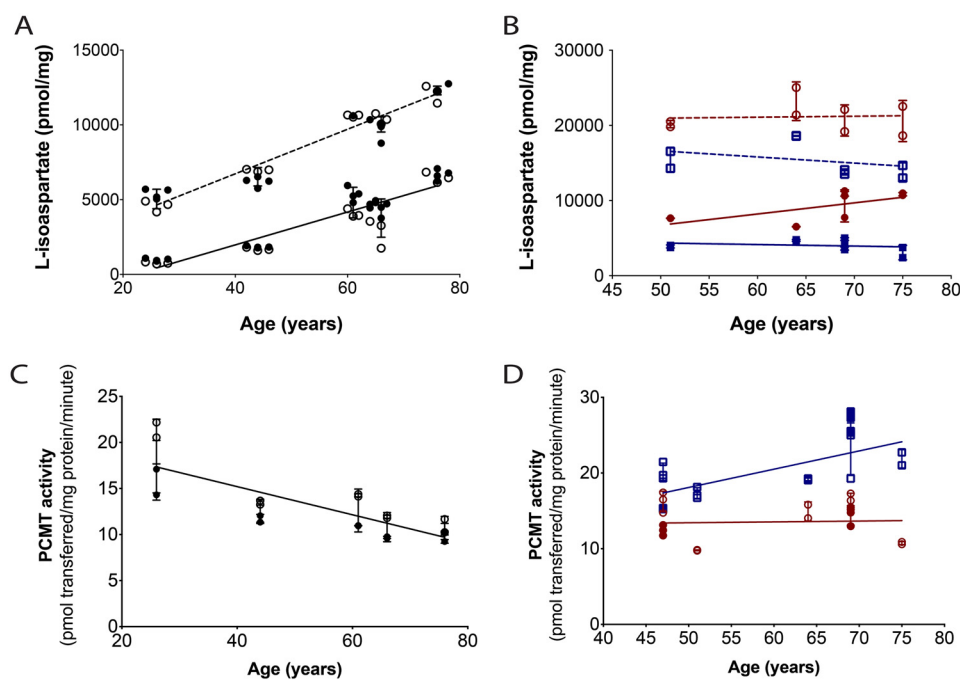
Figure 2. The L-isoAsp modification accumulates to high levels within the aged human lens polypeptides, whereas endogenous methyltransferase repair activity is largely maintained with age. Lens extracts (25 μg of protein) were radiolabeled by 6 μg of PCMT1 and 10 μM [^{3}H]AdoMet for 2 h at 37 °C as described under "Experimental Procedures." *A*, L-isoAsp quantified in whole-lens extracts. *Closed circles*, a single eye lens; *open circles*, the other eye from the same individual. The *solid line* includes the WS extracts; the *dashed line* includes the urea-solubilized WI extracts. Each *symbol* represents one technical replicate. *Error bars*, S.D. of the biological replicates. *Lines* were linear regression fits in GraphPad, and the slope was found to be significantly nonzero for both WS and WI extracts at 0.0048 and 0.0045 p values, respectively. *B*, L-isoAsp levels quantified in dissected lens nuclear (*red circles*) and cortical (*blue squares*) extracts. The *solid line* and closed symbols represent the WS extracts; the *dashed line* and open symbols represent the WI extracts. Each *symbol* represents one technical replicate. *Error bars*, S.D. of the technical replicates. *Lines* were linear regression fits performed in GraphPad, and none of the lines had significantly nonzero slopes (p values were all >0.05). *C*, PCMT1 activity in whole-lens extracts was quantified by detecting the amount of [^{3}H]AdoMet radioactivity transferred to 100 μM peptide substrate KASA(isoD)LAKY by 15 μg of lens extract protein in 2 h at 37 °C. *Closed circles* represent one lens from an individual; *open circles* represent the other lens from that individual. Each *symbol* represents one technical replicate. *Error bars*, S.D. of the technical replicates. In a linear regression fit performed in GraphPad, the slope of the line was significantly nonzero with a p value of 0.0258. *D*, PCMT1 activity in dissected lens nuclear (*red circles*) and cortical extracts (*blue squares*). *Open* and *closed symbols* represent each lens from one individual at 47 and 69 years old. Each *symbol* represents a technical replicate. *Error bars*, S.D. of the technical replicates. *Lines* were linear regression fits performed in GraphPad, and neither of the lines had significantly nonzero slopes (p values were greater than 0.05).

WS extracts in the younger samples and some 2-fold higher in the older samples. Control experiments using the peptide substrate KASA-isoD-LAKY showed that urea content of the WI samples did not affect the PCMT1 activity (Fig. S1).

The nuclear region of the lens develops prior to birth, whereas the cortical region continues to grow throughout an organism's life span. Thus, the interior nuclear sections of the spherical lens are more aged than the exterior cortical regions. To see how L-isoAsp levels compared between these regions, separate lenses from 47–76-year-olds were further dissected into nuclear and cortical regions. The 75-year-old WS dissected lens sample averages 6960 pmol of L-isoAsp/mg of protein extract, whereas the 76-year-old WS whole-lens sample has a mean value of 6590 pmol of L-isoAsp/mg of protein extract, showing that the averages of the aging WS cortex and nucleus correspond well with the values observed in the WS whole-lens extract. The urea-solubilized WI extracts again demonstrated the greatest level of the L-isoAsp modification, and in both the WS and WI extracts, the lens nucleus contained higher amounts than the cortex (Fig. 2B). However, the averages of the WI nucleus and cortex protein extracts were significantly higher than the WI whole-lens protein extracts, with the 75-year-old WI nucleus and cortex averaging 17,200 pmol of L-isoAsp/mg of protein extract, and the 76-year-old WI whole

lens averaging 12,300 pmol of L-isoAsp/mg of protein extract. These variations may be the result of differences in efficiency of urea solubilization of the whole lenses *versus* the dissected lens regions.

The high levels of the L-isoAsp modification— up to 17,200 pmol of L-isoaspartate/mg of protein in the urea-solubilized water-insoluble lens extract– corresponds to an average of ~0.4 isoaspartyl residues per polypeptide chain, indicating that almost half of all proteins in this fraction may be modified. We did not quantify total L-isoAsp within water-insoluble urea-insoluble (UI) fractions due to the inability to fully solubilize this protein fraction in a buffer compatible with the PCMT1 enzyme. This UI fraction has been shown to increase to up to 30% of the fiber cell mass after 50 years of age (26, 27). Thus, within our assays, we may only be quantifying a small portion of the total L-isoAsp within the lens. However, our calculation of 0.4 isoaspartyl residues per polypeptide chain can be taken as a minimal estimate of the total levels of aspartate isomerization within lens proteins.

The L-isoAsp repair enzyme PCMT1 is present in the aging lens and should mediate the accumulation of L-isoaspartyl residues (16). In Fig. 2C, endogenous PCMT1 activity levels between the human 26-year-old and 44-year-old whole-lens extracts were found to decrease from ~18.5 to 12.5 pmol/

min/mg and then remained relatively constant throughout the 61-, 66-, and 76- year-old tissues, reaching a minimum activity of 10.4 pmol/min/mg in the 76-year-old extract. In the dissected nuclear and cortical lens extracts, enzyme activity levels were an average of 7 pmol/min/mg higher within the cortical extracts than the nuclear extracts of the same lens, suggesting that endogenous PCMT1 activity within the nucleus may be affected by the age of the enzyme. However, the levels of PCMT1 activity observed within the 76-year-old whole lens sample and the 51- and 75-year-old nuclear samples are still some 50% of the highest activities in younger lenses. These data show that whereas the activity of the L-isoaspartyl repair enzyme may decrease slightly with age in the human lens, it is still significant within the oldest samples. The lack of PCMT1 repair activity is unlikely to be due to limiting amounts of the AdoMet cofactor, as studies have reported that in the aged nucleus, the minimum level of AdoMet observed is 10 μM (28). Thus, *in vivo*, the repair enzyme may be inhibited by another small molecule or occluded from repairing the L-isoAsp sites, resulting in the accumulation of L-isomerized aspartyl residues seen in Fig. 2 (*A* and *B*).

To investigate the possibility that endogenous PCMT1 may be obstructed from repairing L-isoAsp sites, exogenous PCMT1 activity was tested against soluble and aggregated $\alpha A^{66-80,isoAsp76}$ peptide (SDRDKFVIFL(isoAsp)VKHF). The purified enzyme was able to methylate over 100% of the analyzed soluble peptide, which may indicate that the other aspartate residues within the peptide are partially isomerized (Fig. S2). In contrast, only 2% of analyzed peptide aggregates were observed to be methylated. These results support the hypothesis that the repair enzyme cannot access L-isoAsp sites within heavily aggregated species for repair.

Age-related L-isoaspartyl sites are largely localized to low-molecular weight polypeptides

PCMT1 was again used as an analytical probe with [³H]AdoMet to specifically label and visualize L-isoAsp sites within lens polypeptides by radiolabeling and subsequent SDS-PAGE separation. PCMT1-radiolabeled whole-lens extracts were separated via SDS-PAGE as shown in Fig. 3 (*A* and *B*). The gels were exposed to a film to localize radioactive signals corresponding to polypeptides containing L-isoaspartyl residues. In the fluorographs of whole-lens extracts from the 26-year-old sample, radioactivity is found predominately in the positions corresponding to the molecular weights of the α- ($\sim$19–20-kDa), β- ($\sim$22–28-kDa), and γ- ($\sim$20–21-kDa) crystallins (Fig. 3 (*A* and *B*), *bottom panels*). However, in the older lens samples, there is reduced radioactivity in the crystallin polypeptides, but now significant amounts of radioactivity are present in the extreme high- ($>$200-kDa) and low-molecular weight ($<$14-kDa) regions of the gel. These results suggest that isomerization of crystallins may result in their aggregation to species resistant to SDS denaturation or in their proteolysis.

The localization of L-isoAsp-containing polypeptides to low- and high-molecular weight species seen in the older whole-lens extracts in Fig. 3*A* was also observed in lens samples dissected into nuclear and cortical regions (Fig. 3*B*). Here, we only observed distinct bands corresponding to intact crystallin

molecular weights in the cortical extracts. These results further support the idea that soluble crystallins accumulating isomerized L-aspartate residues may become insoluble or degraded over time in the nucleus of the aged lens.

L-Isoaspartyl–containing polypeptides of high- and low-molecular weight regions from SDS-polyacrylamide gels are localized to the void volume fraction of size-exclusion chromatography

WS whole-lens and nuclear lens extracts were fractionated by size on a native gel filtration column that has a void volume corresponding to proteins of greater than 5000 kDa. Four distinct UV-absorbing peaks were detected, which match those identified by Harding (29): a high-molecular weight (HMW) peak in the void volume, an α crystallin peak, βH/βL crystallin peaks, and a γ crystallin peak (Fig. 4, *A* and *B*). We found that the UV absorbance of the HMW peak in both the whole-lens and the nuclear extracts increases with age in respect to the soluble crystallin fractions, likely correlating to an increase in aggregated protein. When fractions of the whole-lens extracts were analyzed for L-isoaspartyl levels by PCMT1-radiolabeling, little signal was found in the 26- and 44-year-old samples, whereas a large peak of radioactivity was found in the HMW fraction of the 76-year-old extract. In the nuclear extracts, radioactivity is found in all age samples in the HMW and crystallin fractions but does increase with age (Fig. 4*B*). Interestingly, no peak was seen to correspond to very low molecular weights below the γ crystallin peak; nor was damage observed in that region, as might have been expected from the results seen in Fig. 3, where large amounts of L-isoaspartate signal were seen in the LMW region of the SDS-PAGE fluorograph. This result suggests that the low-molecular weight isoaspartyl-containing polypeptides seen on SDS-PAGE are aggregated in the absence of SDS.

To investigate the possibility suggested above, the gel filtration fractions were concentrated by precipitation with TCA, resuspended pellets were radiolabeled by PCMT1 and separated by SDS-PAGE, and the L-isoAsp signal was detected by fluorography in whole-lens samples (Fig. 5) and in nuclear extracts (Fig. S3). TCA precipitation would be expected for peptides of 2 kDa or higher (30). Strikingly, the LMW species observed in Fig. 3 reappear via fluorography within the HMW gel filtration fraction in both whole-lens extracts and nuclear extracts and again show large amounts of the L-isoAsp signal. These LMW species are below the intact weights of the human crystallins, suggesting that they are cleaved fragments that must be aggregated or otherwise interacting with larger protein species.

The aggregated LMW species from the HMW gel filtration fraction represent a variety of lens protein fragments, which accumulate with age and contain isomerization-prone sites

The HMW fractions from the 44-year-old and 76-year-old WS whole-lens samples were resuspended in urea, and LMW species were isolated by passage through a molecular weight cutoff filter as described under "Experimental Procedures." These LMW eluents were analyzed by MS (without any protease treatment) to identify specific endogenous protein fragments against a database of 10 highly abundant lens proteins: αA crystallin, αB crystallin, βA3 crystallin, βA4 crystallin, βB1
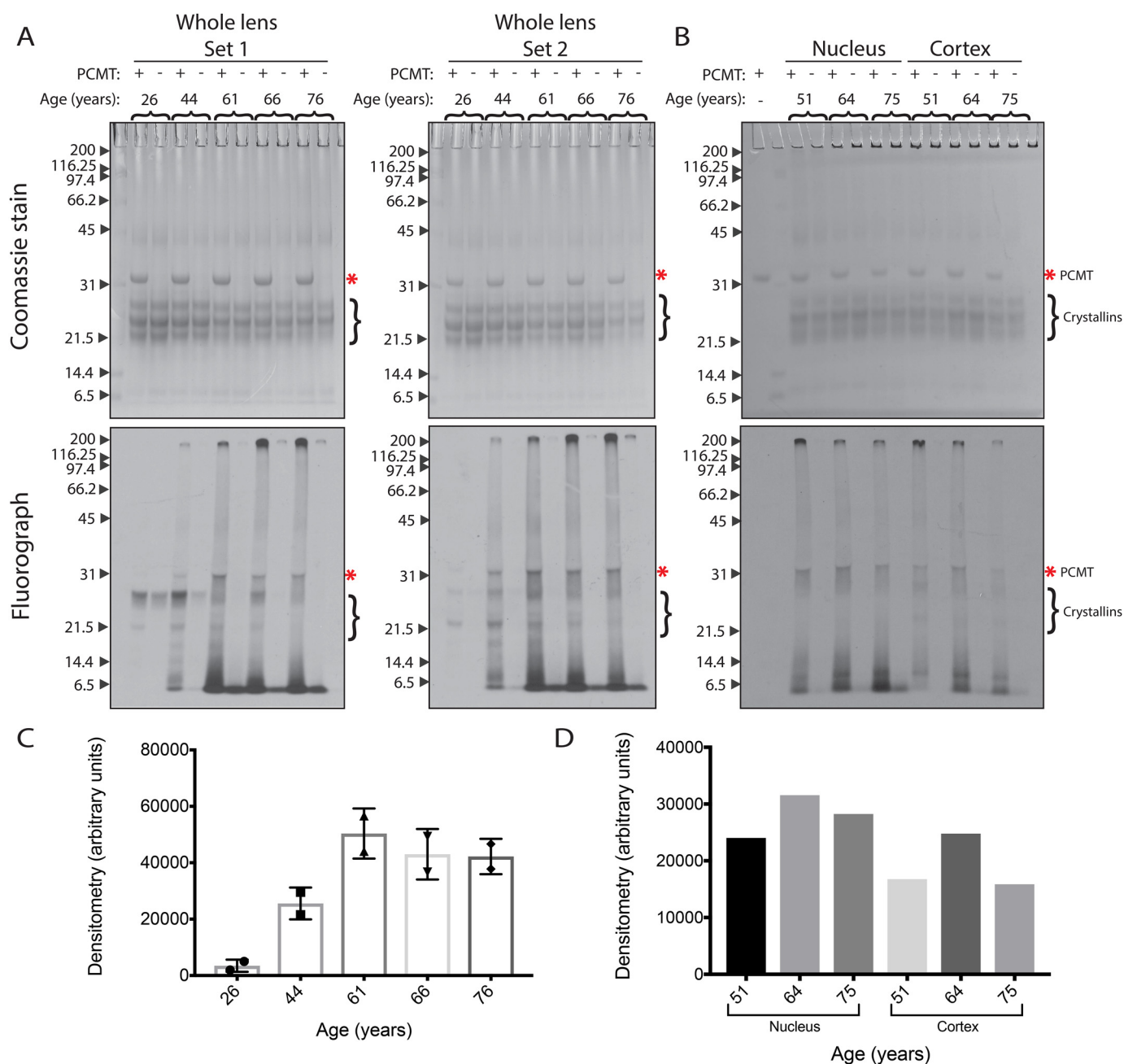
Figure 3. L-isoAsp damage accumulates with age throughout a range of polypeptide sizes in water-soluble extracts of human lenses, primarily within LMW species. WS extracts (25 μg of protein) were incubated with 0.3 μM [^{3}H]AdoMet and with (+) or without (−) 5 μg of PCMT1 for 2 h at 37 °C, and polypeptides were analyzed by SDS-PAGE using a 12% acrylamide matrix. Coomassie-stained gels are shown at the *top*; fluorographs (2-day exposures) are shown at the *bottom*. Molecular weight markers (kDa) are indicated with *arrows* to the left of each gel and include myosin, β-gal, phosphorylase b, BSA, ovalbumin, carbonic anhydrase, soybean trypsin inhibitor, lysozyme, and aprotinin (Bio-Rad SDS-PAGE Molecular Weight Standards, Broad Range, catalogue no. 161-0317). The band corresponding to PCMT1 is indicated by *asterisks*. The migration positions of intact crystallins are indicated by *brackets* on the *right-hand side* of the gels. *A*, whole-lens extracts from two lenses of each individual. *B*, nuclear and cortical separated extracts from a single lens (1-day exposure). *C*, densitometry of lanes from whole-lens sets 1 and 2. *Error bars*, S.D. of the two lanes. *D*, densitometry of lanes from nuclear and cortical sets.

crystallin, βB2 crystallin, γC crystallin, γS crystallin, filensin, and phakinin. Peptide fragments were identified from all of these proteins, although only one peptide was identified from γC crystallin. All peptides with an ion score of 26 or higher are shown in Tables S1–S9, whereas the top five peptides as ranked by ion score of each protein are represented in Table 2. Of the proteins, αA crystallin, αB crystallin, filensin, and phakinin had the highest numbers of identified peptide sequences, perhaps reflecting high levels of these lens protein fragments within the

WS-HMW aggregates. The sequence coverage of each of the 10 proteins is shown in Table 1. The frequency of specific residues at the N and C termini of all of the protein fragments combined is represented in Fig. 6A. Although there is not a strong occurrence of any one residue at the termini, the most frequent residues found at the N termini were Ser, Arg, and Gly residues, whereas at the C terminus Leu, Gln, Lys, and Phe residues were most abundant (Fig. 6A). Notably, neither Asn nor Asp was prevalent at the termini, which suggests that nonenzymatic
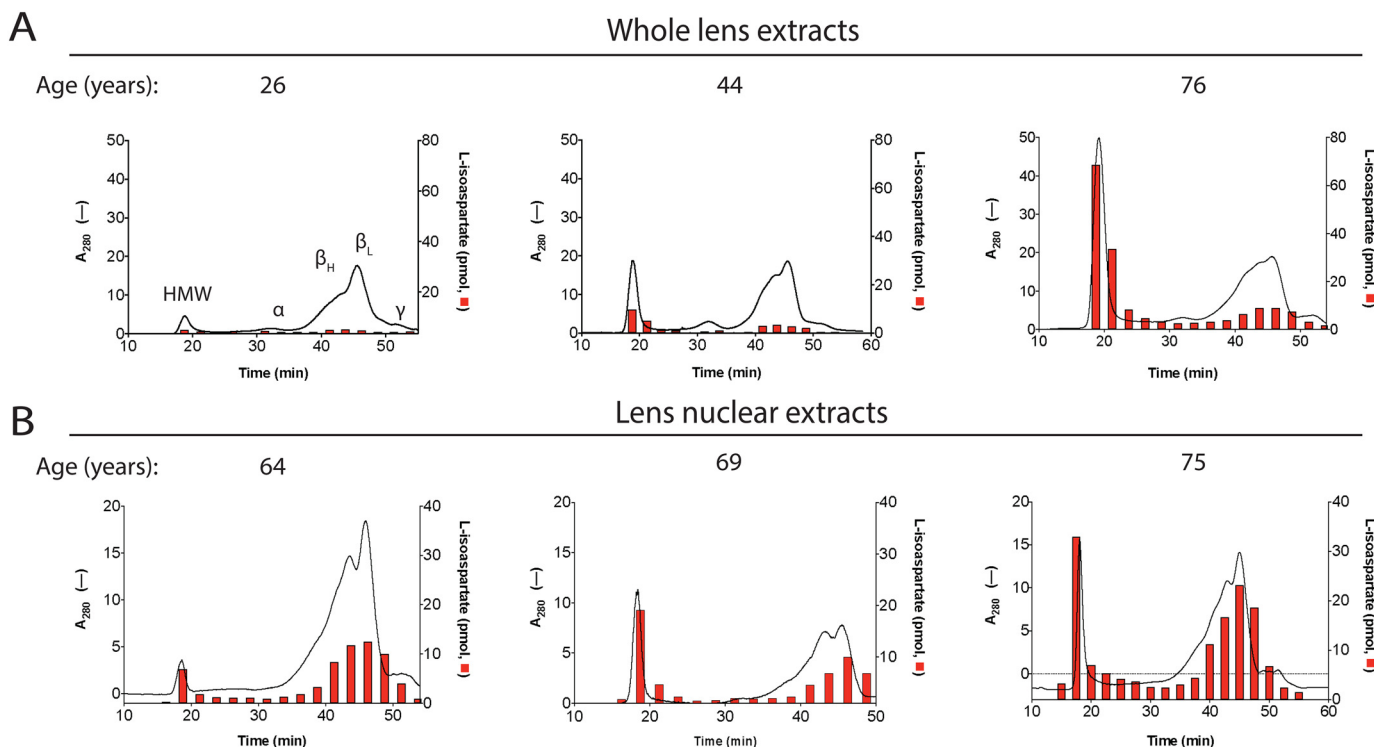
Figure 4. Size-exclusion chromatography of WS extracts demonstrates age-dependent increases in HMW protein species and in L-isoAsp damage in crystallins, particularly within the HMW fractions. One mg of lens extract was loaded onto a 24-ml Superose 6, 10/300 GL gel filtration column, and proteins were eluted at 0.4 ml/min in 50 mM Tris-HCl, pH 7.9, 150 mM NaCl. One-ml fractions were collected, and 25 μl of each fraction was removed for L-isoAsp quantification (*red columns*) as described under "Experimental Procedures." The *black lines* represent UV absorbance at 280 nm. Peaks were defined throughout as *labeled* in the *26-year-old panel*. These designations are based on the known molecular weights of α- and β-crystallin oligomers, coupled with the void volume of the column. *A*, whole-lens extracts; *B*, nuclear extracts. The age of the lens in years is designated at the *top* of each corresponding graph.
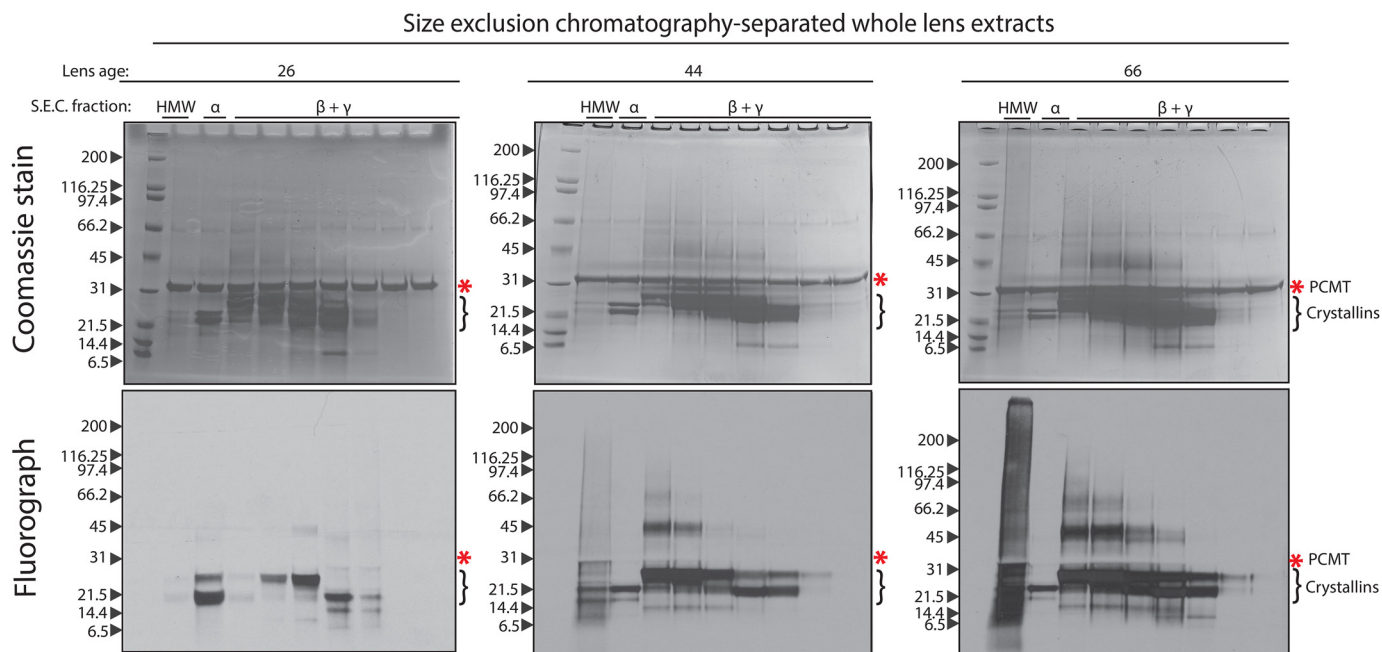
Figure 5. Analysis of L-isoAsp damage in the native size-exclusion fractions of human whole-lens extracts by SDS-PAGE reveals that the HMW gel filtration fraction contains significant amounts of LMW L-isoaspartyl– containing species. Fractions from size-exclusion chromatography as in Fig. 4 were TCA-precipitated and resuspended in 100 mM Tris-HCl, pH 7.9, 150 mM NaCl, 0.1% SDS, 6 M urea, and L-isoAsp sites within the fractions were radiolabeled by PCMT1 and [³H]AdoMet as described in the legend to Fig. 3. Labeled fractions were then separated by SDS-PAGE on a 4–12% gradient gel. The Coomassie-stained gel is shown in the upper panels; the fluorograph (1-week exposure) is shown in the *bottom panels*. The bands corresponding to PCMT1 in the Coomassie-stained gel are indicated by *asterisks*. The migration positions of intact crystallins are indicated by *brackets* on the *right-hand side* of the gels. Labels *above* the lanes represent the corresponding peaks from the size-exclusion run (see Fig. 4). The age of lens sample in years is designated *above* the corresponding gel.

Table 1

Parent proteins of lens fragments

Lens peptides were isolated from the gel filtration HMW fraction and identified as described under "Experimental Procedures" against the 10 proteins in the table below. The sequence coverage and number of unique peptides are reported for the 44-year-old and 76-year-old lens samples.

Accession no.	Description	Coverage (%)	No. of unique peptides
P02489	α crystallin A	75	74
P02511	α crystallin B	78	54
P05813	β crystallin A3	55	15
P53673	β crystallin A4	57	24
P53674	β crystallin B1	52	31
P43320	β crystallin B2	67	25
Q12934	Filensin	30	73
P07315	γ crystallin C	5	1
P22914	γ crystallin S	47	15
Q13515	Phakinin	46	68

cleavages via the succinimide ring intermediate are not common within the aged WS extract (31).

The relative abundances of the peptide fragments were quantified to see which peptides increased between the 44- and 76-year-old samples (Table 2; Tables S1–S9). A majority of these peptides increase in abundance in the 76-year-old sample. In Fig. 6B, the sites of cleavage for αA and αB crystallin were mapped onto a diagram of the domains of these crystallins. Although there are a higher absolute number of cleavages within the core α crystallin domain, there are also a significant number within the terminal domains. Together, these results suggest that there is no strong sequence specificity of the crystallin fragmentation of αA and αB crystallin in the WS aggregates, but that the α crystallin domain of the proteins may be more accessible to cleavage due to the involvement of the terminal domains in oligomerization of the crystallins (32). There are, however, strong biases within the βA4 crystallin, βB1 crystallin, βB2 crystallin, and filensin proteins. The majority of fragments observed for these proteins are from the C terminus, perhaps indicating that these are derived from truncations of the proteins (Tables S4–S7).

Isomerized forms of MS-identified peptides αA$^{52-65}$ and αA$^{89-98}$ modestly increase protein precipitation

Of the 38 peptides with an ion score of 26 or higher identified from αA crystallin, 34 were found to contain at least one of the following aspartate residues: Asp^{58}, Asp^{67}, Asp^{76}, Asp^{84}, Asp^{91}, Asp^{92}, and Asp^{136}. All of these sites, excepting 67 and 136, have been shown in previous literature to be highly isomerized, particularly Asp^{58} and Asp$^{91/92}$ (19, 23), which lie in the N-terminal region and the α crystallin domain, respectively. To investigate the possible effects of L-isoaspartate accumulation in short peptides within the water-soluble extract of the aging lens, we used synthetic peptides of two αA crystallin peptides that were identified from the WS-HMW peak by MS (Table S1), ^{52}LFRTVLDSGISEVR^{65} (αA$^{52-65}$) and ^{89}VQDDFVEIH^{98} (αA$^{89-98}$), with the L-isoaspartate modification introduced at Asp^{58} (αA$^{52-65,isoAsp58}$) and Asp^{91} (αA$^{89-98,isoAsp91}$), respectively.

The α crystallins are related to small heat-shock proteins and act as molecular chaperones within the lens, suppressing aggregation of misfolded crystallins (33). To see the effect of these peptides on the chaperone activities of αB crystallin, the αA crystallin segments were first incubated with purified αB crys-

tallin and alcohol dehydrogenase (ADH) under conditions that cause ADH to denature and aggregate. The ability of αB crystallin to prevent ADH aggregation was then monitored over time by light scattering at $A_{360\,nm}$. In Fig. 7A, the aggregation of ADH is largely prevented by the addition of chaperone αB crystallin, as shown by the significant reduction in light scattering. Neither the addition of the αA$^{52-65,isoAsp58}$ nor the αA$^{89-98,isoAsp91}$ peptide appears to alter the levels of aggregation when added to ADH with αB crystallin. Thus, inhibition of the activity of the αB crystallin chaperone by the isomerized peptides was not observed under these conditions.

To probe the peptides' effects on crystallin solubility, two different amounts of αA$^{52-65,isoAsp58}$ and αA$^{89-98,isoAsp91}$ peptides were then incubated with the 47-year-old WS nuclear extract. After centrifugation, the pellets were solubilized and separated by SDS-PAGE (Fig. 7B). Increases in the amount of protein in the pellet were seen when both 25 and 50 μg of the peptides were present as quantified by densitometry (Fig. 7C). Thus, the addition of the isoaspartyl-containing peptides, especially αA$^{89-98,isoAsp91}$, may modestly promote insolubilization of the lens proteins.

The isomerized αA$^{52-65,isoAsp58}$ peptide shows decreased self-aggregation and lens protein precipitation compared with the native αA$^{52-65}$ peptide

The αA$^{52-65}$, αA$^{52-65,isoAsp58}$, and αA$^{89-98,isoAsp91}$ peptides were all soluble at physiological pH, whereas the native αA$^{89-98}$ could only be solubilized in 3% ammonium hydroxide. To facilitate comparison between native and isomerized peptides, the αA$^{52-65}$ peptides were solubilized in Tris buffer, and the αA$^{89-98}$ peptides were solubilized in ammonium hydroxide as described under "Experimental Procedures." Whereas none of the peptides were observed to bind thioflavin T (ThT), self-aggregation of the native and isomerized forms was monitored by light scattering at 340 nm (Fig. 8A). The only peptide to show significant increases in light scattering as a result of precipitation was the native αA$^{52-65}$ peptide.

We observed in the previous experiment that the isomerized peptides were able to induce moderate increases in precipitated lens proteins. To investigate the effects of the isomerized peptides relative to the native forms, the αA$^{52-65}$ and αA$^{52-65,isoAsp58}$ peptides were incubated with 47-year-old WS nuclear extract. The αA$^{89-98}$ peptides were not used due to the high alkaline conditions required for solubilization of the native peptide, which alone may affect lens protein stability. In Fig. 8B, the increases in protein levels within the precipitated pellet with the native αA$^{52-65}$ peptide can be readily visualized. Densitometry analyses of these gel lanes again show limited increases in protein with the αA$^{52-65,isoAsp58}$ peptide, but more significant shifts are observed with the native αA$^{52-65}$ peptide (Fig. 8C).

The previously identified WI-derived αA crystallin peptide ^{66}SDRDKFVIFLDVKHF^{80} displays enhanced amyloid formation and precipitation of αB crystallin in vitro upon the introduction of L-isoAsp at Asp^{76}

The αA crystallin ^{66}SDRDKFVIFLDVKHF^{80} (αA$^{66-80}$) anti-chaperone peptide fragment was previously shown to accumulate within WI lens extracts (34). Our MS of WS-HMW pep-
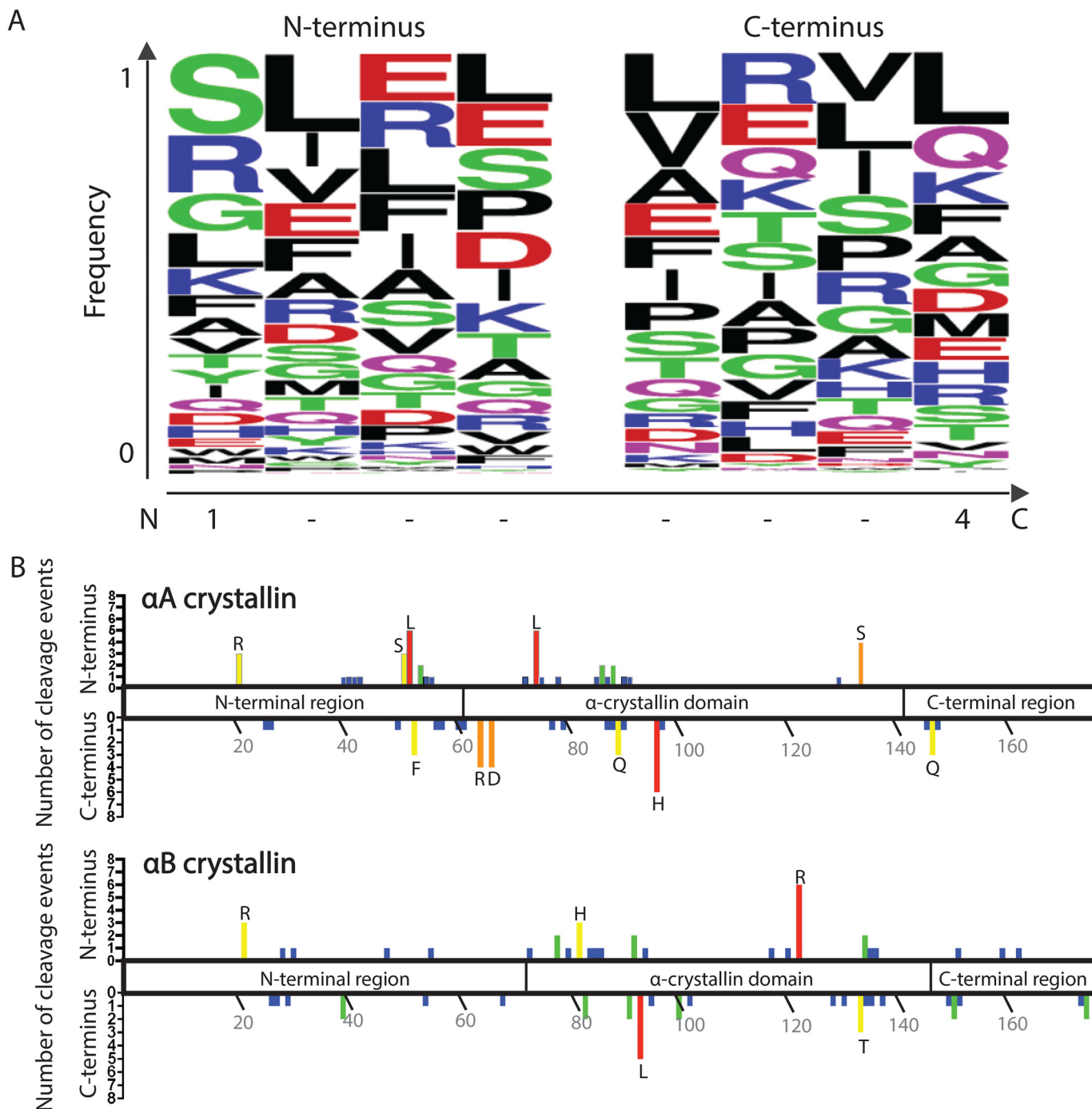
Figure 6. The identified WS-HMW protein fragments do not display distinctive patterns at N or C termini, nor a strong localization of cleavage sites. *A*, the four amino acid residues present at the N- and C-terminal sequences of all peptides identified by MS in the WS-HMW fraction were inputted into WebLogo. The *y* axis represents the fraction of a particular residue that occurs at the indicated position. On the *x* axis, position 1 of the N terminus represents the first residue of the cleaved peptide, whereas position 4 of the C terminus represents the last residue of the cleaved peptide. *B*, graphical representation of the cleavage sites observed in WS-HMW peptides along the domains of αA crystallin (*top*) and αB crystallin (*bottom*). The *upper y* axis represents the number of times the residue indicated on the *x* axis was found at the N terminus of peptides. The *lower y* axis represents the number of times the residue indicated on the *x* axis was found at the C terminus of peptides. Residues with three or more cleavages are designated by their single-letter amino acid code.

tides showed overlapping fragments in this region of αA, but the full αA$^{66-80}$ was not found (Table S1). Isomerization at the Asp^{76} within αA crystallin has been demonstrated previously (19, 23). We were thus interested in the effects of isomerization of the αA$^{66-80}$ peptide on its aggregation and anti-chaperone activity. We show in Fig. 9*A* that a synthetic αA$^{66-80}$ peptide containing L-isoAsp at Asp^{76} (αA$^{66-80,isoAsp76}$) demonstrates

increased rates of aggregate formation compared with the unmodified peptide as measured by ThT fluorescence. The peptides were incubated in buffer without ThT, and resultant fibers are shown in Fig. 9*B*. Thus, *in vitro*, the peptides are forming ordered, fibrillar aggregates.

The αA crystallin peptides were then incubated with αB crystallin and ADH under conditions that cause ADH to dena-

Table 2

Top five peptides identified from each of 10 abundant lens proteins

Lens peptides were isolated from the gel filtration HMW fraction and identified as described under "Experimental Procedures." The five peptides with the highest ion scores from each of the proteins listed in Table 1 are displayed with their corresponding theoretical mass and relative abundances in a 44-year-old and 76-year-old whole-lens sample on a scale of 0–200.

Parent protein	Sequence	Theoretical MH$^+$ (Da)	Relative abundances	
			44-Year-old	76-Year-old
αA crystallin	^{52}LFRTVLDSGISEVR^{65}	1591.88023	2.2	197.8
	^{56}VLDSGISEVR^{65}	1074.57896	12.9	187.1
	^{134}SADGMLTFCGPKIQ^{147}	1524.71851	6	194
	^{54}RTVLDSGISEVR^{65}	1331.72775	68.3	131.7
	^{51}SLFRTVLDSGISEVR^{65}	1678.91226		200
αB crystallin	^{93}VLGDVIEVH^{101}	980.54112	57.2	142.8
	^{29}GEHLLESDLFPT^{40}	1357.66342	9.8	190.2
	^{123}RIPADVDPLTIT^{134}	1310.73144	2.2	197.8
	^{123}RIPADVDPLTITS^{135}	1397.76347	2.7	197.3
	^{95}GDVIEVH^{101}	768.38864		200
βA3 crystallin	^{29}GPWKITIYD^{37}	1092.57242	200	
	^{152}GWFNNEVGSMKIQ^{164}	1509.71547		200
	^{127}TIFEKENFIGRQ^{138}	1481.7747	16	184
	^{124}SKMTIF^{129}	726.38547	1.4	198.6
	^{139}WEISDDYPSLQAM^{151}	1554.67809	0.4	199.6
βA4 crystallin	^{108}TIFEQENFLGKK^{119}	1453.76856		200
	^{109}IFEQENFLGKK^{119}	1352.72088	1.4	198.6
	^{120}GELSDDYPSLQAM^{132}	1425.62024	1.8	198.2
	^{105}SRLTIFEQENFLGKK^{119}	1809.98576		200
	^{104}DSRLTIFEQENFLGKK^{119}	1925.0127		200
βB1 crystallin	^{238}HLEGSFPVLA^{247}	1069.56767		200
	^{238}HLEGSFPVLATEPPK^{252}	1621.85843	21	179
	^{240}EGSFPVLATEPPK^{252}	1371.71546	2.3	197.7
	^{242}SFPVLATEPPK^{252}	1185.6514	54.3	145.7
	^{38}TLAPTTVPITSAK^{50}	1299.75184	22.2	177.8
βB2 crystallin	^{121}KMEIIDDDVPSFHAH^{135}	1753.8214		200
	^{121}KMEIIDDDVPSFHA^{134}	1616.76248		200
	^{121}KMEIIDDDVPSFHAHG^{136}	1810.84286		200
	^{122}MEIIDDDVPSFHAH^{135}	1625.72643		200
	^{143}SVRVQSGTWVGYQYPGYRGL^{162}	2273.14618		200
Filensin	^{79}GELAGPEDALARQVE^{93}	1554.77583	66.3	133.7
	^{324}FIETPIPLFTQSH^{336}	1529.79986		200
	^{239}RVELQAQTTTLEQAIK^{254}	1829.0127	5.8	194.2
	^{324}FIETPIPLFTQ^{334}	1305.70892	1.1	198.9
	^{191}QQIIHTTPPASIVTS^{205}	1592.86425	2.6	197.4
γS crystallin	^{60}YILPQGEYPEYQRWM^{74}	1972.9262		200
	^{98}IFEKGDFSGQ^{107}	1127.53677		200
	^{65}GEYPEYQRWM^{74}	1358.5834	13.2	186.8
	^{50}YERPNFAGYM^{59}	1247.55137		200
	^{98}IFEKGDFSGQMYETTED^{114}	1996.84806	10	190
Phakinin	^{162}QQVGEAVLENARL^{174}	1426.76487		200
	^{157}WASSCQQVGEAVLENARL^{174}	2017.976		200
	^{211}KVIDEANLTKM^{221}	1261.68205	6.3	193.7
	^{266}TGLDDILETIRIQ^{278}	1486.81115		200
	^{162}QQVGEAVLENARLM^{175}	1557.80535	4	196
γC crystallin	^{166}SLRRVVDLY^{174}	1120.64732		200

ture, which was monitored by light scattering at $A_{360\,nm}$. In Fig. 9C, the light scattering of ADH alone plateaus at ~0.5 absorbance units. When the chaperone αB crystallin is introduced, the level of light scattering is significantly reduced. However, when the αA anti-chaperone peptide is introduced, the levels are similar to ADH alone. When the L-isoAsp–modified αA segment is used, the levels rise over those of ADH alone. This is unlikely to be due to extra scattering by the aggregation of the peptide with itself, as this yields relatively low light scattering (Fig. 9D). However, when the peptide is incubated with αB crystallin alone, there is significant light scattering (Fig. 9D). We tested the peptides' abilities to aggregate the chaperone at lower concentrations and found that as little as 5 μg of L-isoAsp modified peptide to 40 μg of αB crystallin was sufficient to cause light scattering (Fig. S4). Thus, the inhibition of αB crystallin's chaperone abilities may not be entirely direct, but rather an increase in the aggregation of the chaperone itself, exacerbated by the L-isoAsp modification in the α crystallin fragment.

Discussion

In this study, we aimed to establish the extent and potential repercussions of the isomerization of asparaginyl and aspartyl residues across the human lens proteome using highly sensitive and specific radiolabeling of modified residues by PCMT1 with [³H]AdoMet. This method revealed that the L-isoAsp modification in the aged lens localizes to aggregates that elute above 670 kDa on native gel filtration but is found there in low-molecular weight peptide species after SDS-PAGE. Roy and Spector (35) previously demonstrated that WS-HMW species were identical to the insoluble protein fraction in human lenses, with the only distinction being the size of the particles still in suspension. Remarkably, they also found that a major component of these HMW protein fractions appeared to be degraded polypeptides near 11 kDa (35). It has since been determined that crystallin fragments ranging in size between 2.8 and 18 kDa can comprise up to 14–27% total protein content in WS-HMW aggregates of aged and cataract lens extracts (36–38). Our MS

ASBMB

J. Biol. Chem. (2019) 294(32) 12203–12219 **12211**
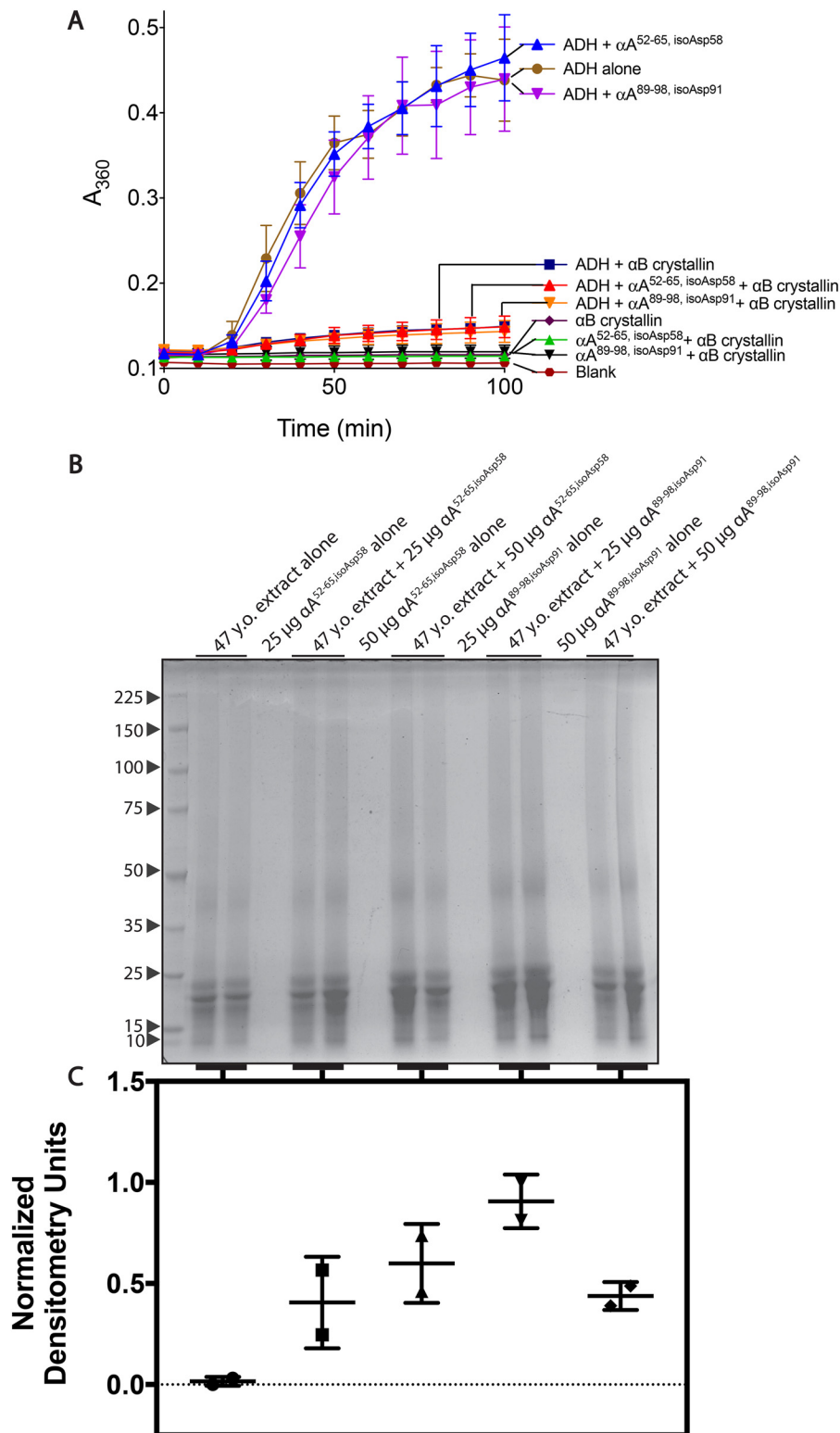
Figure 7. The isomerized forms of WS-HMW derived synthetic peptides $\alpha A^{52-65,isoAsp58}$ and $\alpha A^{89-98,isoAsp91}$ do not inhibit αB crystallin chaperone activity, but modestly increase protein precipitation *in vitro*. *A*, inhibition assays were performed as described under "Experimental Procedures." Briefly, ADH (125 μg) was incubated under denaturing conditions (50 mM sodium phosphate, pH 7.0, 100 mM NaCl, and 10 mM phenanthroline) with and without αB crystallin (50 μg) and peptides (50 μg). Aggregation was monitored by light scattering at $A_{360\,nm}$. *Symbols* represent the mean and *error bars* represent the S.D. of three technical replicates. *B*, 47-year-old lens extract (500 μg) was incubated with both 25 and 50 μg of the $\alpha A^{52-65,isoAsp58}$ or $\alpha A^{89-98,isoAsp91}$ peptides (from stocks made in water) for 14 h at 37 °C. Reactions were spun for 10 min at 3000 rpm. The resulting pellet was separated by SDS-PAGE. Molecular weight markers (kDa) are indicated with *arrows* to the *left* of the gel (Perfect Protein Markers, 10–225 kDa, Millipore Sigma, catalogue no. 69079). *C*, the lanes of the gel were quantified by densitometry and normalized from 0 to 1 based on the lowest and highest values. *Error bars*, S.D. of two replicates.
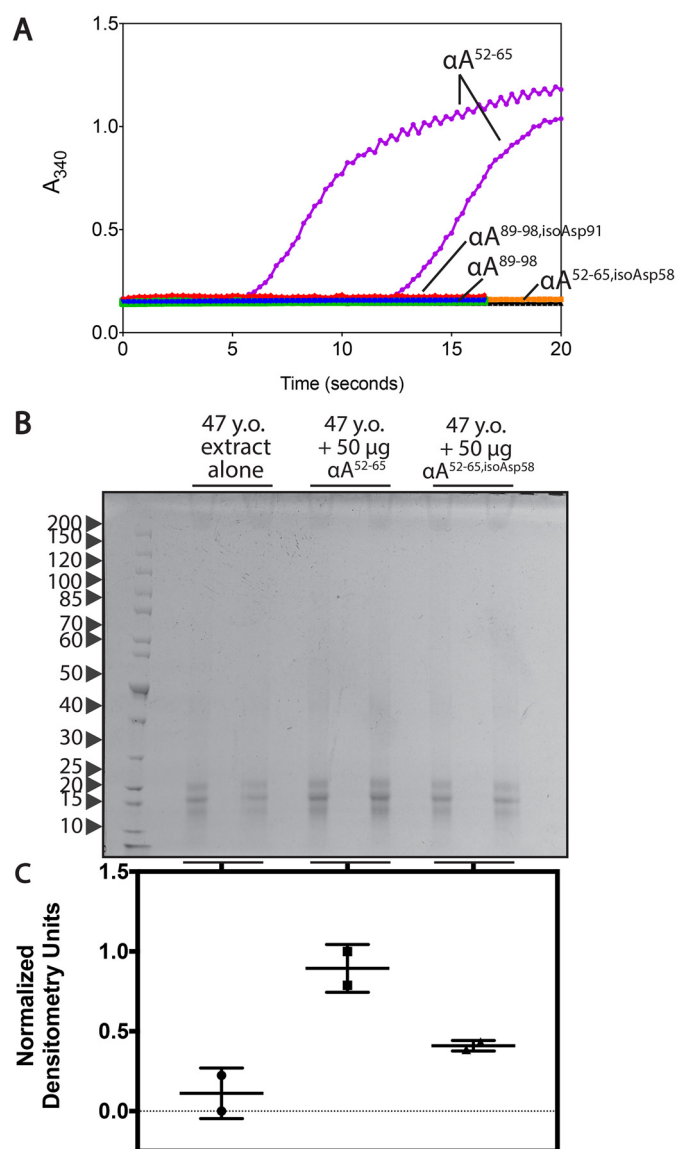
Figure 8. The native form of WS-HMW–derived synthetic peptide αA$^{52-65}$ shows enhanced self-aggregation and protein precipitation compared with the isomerized form. *A*, the isomerized and native αA$^{52-65}$ peptides were dissolved in 50 mM Tris-HCl, pH 7.5, and 1% DMSO at 3 mg/ml. To solubilize the native αA$^{89-98}$ peptide, the isomerized and native forms were first dissolved in 3% ammonia in water as described under "Experimental Procedures" and subsequently diluted into in 50 mM Tris-HCl, pH 7.5, at a final concentration of 2 mg/ml. Aggregation was analyzed by light scattering at 340 nm. Assays were performed in duplicate, and one line for each duplicate is shown. Lines pertaining to peptide solutions are *labeled*; the *black line* represents the buffer background for the αA$^{52-65}$ condition, whereas the *green line* represents the buffer background for the αA$^{89-98}$ condition. *B*, 47-year-old lens extract (500 μg) was incubated with 50 μg of the αA$^{52-65}$ peptides (from stocks made in water) for 14 h at 37 °C. Reactions were spun for 10 min at 3000 rpm. The resulting pellet was separated by SDS-PAGE. Molecular weight markers (kDa) are indicated with *arrows* to the *left* of the gel (PageRuler Unstained Protein Ladder, 10–200 kDa, ThermoFisher Scientific, catalogue no. 26614). *C*, the lanes of the gel were quantified by densitometry and normalized from 0 to 1 based on the lowest and highest values. *Error bars*, S.D. of two replicates.

results reveal the presence of endogenous short peptides in the WS-HMW native gel filtration void volume fraction from 10 different lens proteins (Table 2 and Tables S1–S9). The mechanisms by which these fragments are produced are not fully understood. Due to the presence of fragments cleaved at spe-

cific sites and truncated crystallins during aging, it is believed that some protease activity remains in the lens during aging and slowly degrades the crystallin proteins (39–42).

Previous work shows αA and αB crystallins to be extensively truncated, and some hot spots have been identified, such as between Asp^{129} and Pro^{130} in αB (43, 44). Two αB peptides identified within the work presented here have N- or C-terminal cleavage at or near the Asp^{129}–Pro^{130} bond, including RIPADVD and RIPADVDPL (Table S2). More recently, MALDI tissue imaging was performed on lenses of different ages, identifying intact crystallin fragments in both the nuclear and cortical regions of the tissue (45). The smallest peptide identified in that study was αA crystallin 1–34 (4265 Da), whereas the largest αA peptide identified in the work presented here corresponds to residues 130–147 (1,971 Da). Thus, there were no exact matches in identified peptides. However, several residues found at the C terminus of truncated products overlapped between this study and the MALDI-imaging results, including Gln^{50}, Asp^{58}, Arg^{65}, and Phe^{80}. Arg^{65} appears repeatedly within the peptides presented here and in all cases is more abundant in the 76-year-old sample than the 44-year-old one. The consistent identification of truncation sites between studies may highlight their susceptibility to truncation.

Interestingly, Harrington *et al.* (44) found that the WS-HMW fraction of normal aged lenses contained primarily fragments of αA and αB crystallin, whereas cataractous lenses also had βA3 and βB1 crystallin fragments. In the work presented here, Tables S3 and S5 list five and 16 peptides of βA3 and βB1 crystallin, respectively. All of the βB1 peptides are higher in abundance within the 76-year-old sample, including eight that occur only within this aged sample, whereas four of the five βA3 increase within the 76-year-old sample. This information parallels literature that has shown that over half of deamidations within the insoluble protein fraction of aged lens were found in the β crystallins, particularly βA3 and βB1 (7). From this study, we know that residues Asn^{108} of βB1 and Asn^{133} of βA3 have mass shifts of +1 Da each. Although the mass shift does not reveal whether the product of the deamidation is Asp or isoAsp, both Asn108 of βB1 and Asn133 of βA3 were found to be contained in peptides identified in our study, and these peptides should be examined for the effects of isomerization. Therefore, the βA3 and βB1 peptides identified here, which increase with age, may be significant formations for loss of transparency in both aged and cataractous lenses.

Previous studies have investigated the possible combinatorial effects of truncations and proteolysis on the properties of crystallins, including βB1 and γS. In the case of βB1, the combination of deamidation and truncation had the most severe effects on protein stability, whereas truncation alone had little effect; however, deamidation has not been examined in short βB1 peptides (46). Similarly, isolated N- and C-terminal domains of human γS crystallin showed high heat and pH stabilities (47). Thus, truncated crystallin monomers may be relatively stable. However, it is known that truncation of the β crystallins affects assembly formation, which may in turn affect lens transparency (48). A number of other studies have investigated the effects of shorter fragments produced by truncations on protein aggregation *in vitro* and found that peptides derived
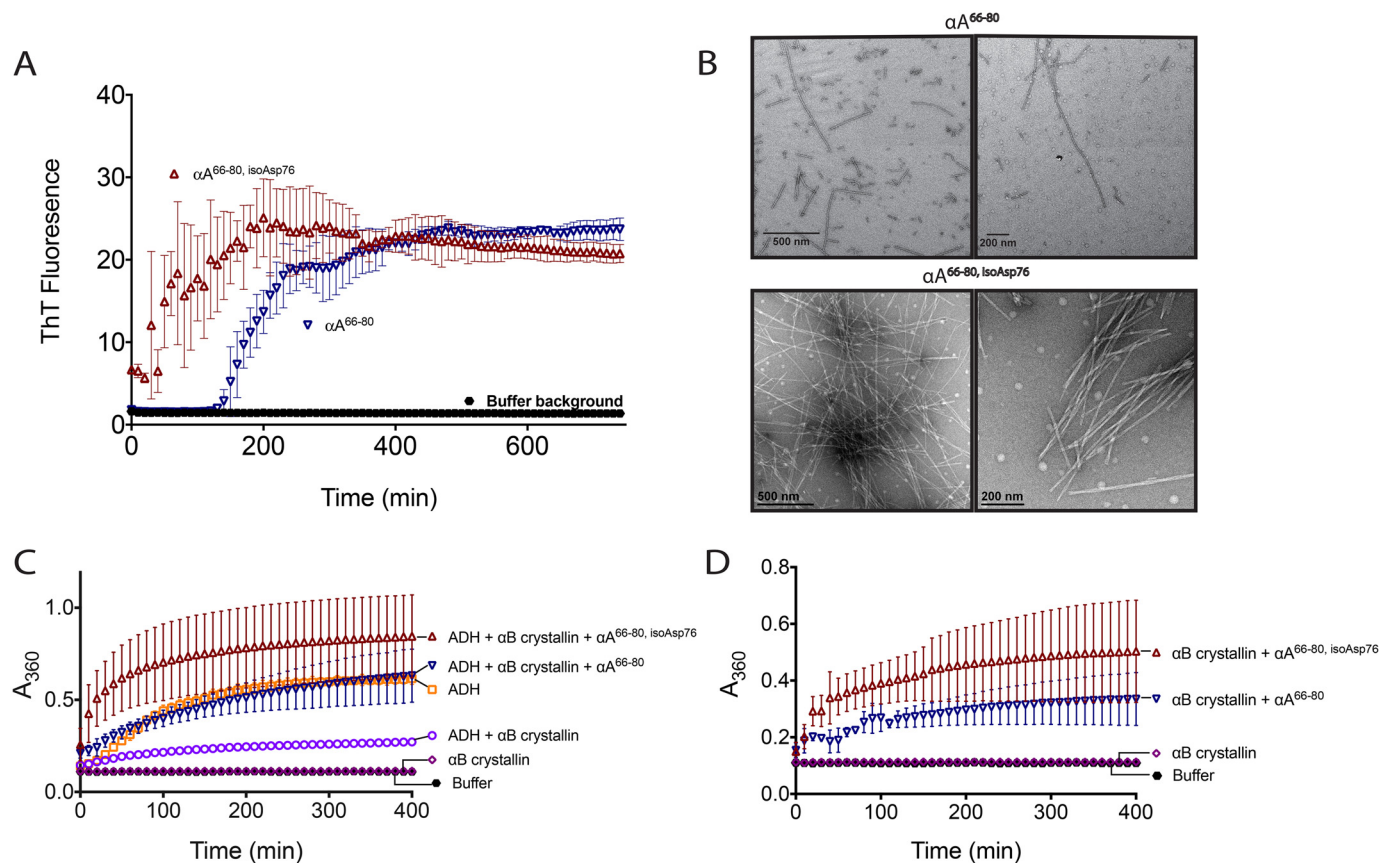
Figure 9. Isomerization of the anti-chaperone peptide αA^{66-80} increases its ability to form amyloid and enhances its anti-chaperone activity *in vitro*. *A*, αA^{66-80} ($\triangledown$) and $\alpha A^{66-80,isoAsp76}$ ($\triangle$) peptides were incubated with amyloid-binding dye thioflavin T to monitor self-aggregation as described under "Experimental Procedures." *B*, peptides were incubated without ThT, and the resulting aggregates were observed by EM as described under "Experimental procedures." *Scale bar*, either 200 or 500 nm, as indicated. Two representative fields are shown. *C*, aggregation was measured for ADH (150 μg) incubated under denaturing conditions (50 mM sodium phosphate, pH 7.0, 100 mM NaCl, and 10 mM phenanthroline) with and without αB crystallin (40 μg) and peptides (40 μg). Aggregation was monitored by light scattering at $A_{360\ nm}$. *D*, control aggregation reactions were performed as in *C* with peptides (40 μg) and αB crystallin (40 μg) alone. Data sets from *C* and *D* were from a single experiment and were separated onto two graphs for clarity; the αB crystallin alone and buffer background from *C* and *D* are duplicated. *Error bars*, S.D. of three replicates.

from both αA and βL crystallins can act as anti-chaperones, interfering with the action of intact αA and αB crystallins against protein misfolding, or as mini-chaperones promoting stability of other proteins (34, 49, 50). A majority of these studies have focused on the unmodified sequences of these crystallin fragments.

Most of the peptides identified within our WS-HMW native gel filtration void volume fraction contained Asp residues that are known to isomerize in the aging lens (23, 51) (Tables 1 and 2 and Tables S1–S9). Our studies of two peptides found in this fraction showed that whereas the L-isoAsp peptides could modestly promote protein precipitation, the native peptides had more severe solubility and aggregation properties. Thus, it appears that the L-isoAsp residue within these two WS-HMW–derived peptides actually decreases their propensities for self-aggregation and protein precipitation. In contrast with these results, we found that for a WI-derived anti-chaperone peptide, the L-isoAsp form showed increased levels of self-aggregation over the L-Asp peptide, as well as increased precipitation of the lens chaperone αB crystallin. It is important to note that whereas we demonstrated that the aggregates of the peptide alone were amyloid in nature, amyloid structures have not definitively been demonstrated within the human lens, but

these may be representative of other forms of aggregation *in vivo* (52). Thus, the effects of the L-isoAsp modification within cleaved peptides can be variable.

Our current work does not fully resolve the fundamental question of how this aspartyl isomerization affects cataract formation. Truscott and Friedrich (11) emphasized the difficulties of establishing causative relationships between specific posttranslational modifications and the opacification of the lens. It is conceivable that modification of an intact enzyme by isoaspartyl formation may affect its activity as reviewed by Reissner and Aswad (54). On the other hand, it could be that for many enzymes or other structural lens proteins, where the modification is not near the active site, isomerization may be benign. However, it could well be that isomerization of the peptides may lead to aggregation, or such peptides may serve as inhibitors of a particular enzyme or as a seed for aggregation of other proteins.

In the molecular heterogeneity of the lens, protein fragments will be interacting and aggregating with other species in complex manners. In these cases, it is too early to predict the effects of the isomerization based solely on the sequence of the damaged peptide. However, in the experiments conducted here, we see a correlation between propensity for self-aggregation and

the precipitation of other proteins (Figs. 8 and 9). Thus, if a peptide is predicted to have higher self-aggregative properties, then it may be more likely to aid in the precipitation of other proteins.

Here we have only presented three cases of isomerization within lens peptides. Therefore, it is difficult to definitively extend these results to other peptide sequences. However, some theories concerning the propensity to self-aggregate can be put forth combining the peptide work presented here with previous literature. Assuming amyloid as a model of self-aggregation, the interdigitation of amino acid side chains is crucial for the formation of the steric zipper and is highly sequence-dependent (53). Thus, the isomerization of an aspartate or asparagine in the core of a steric zipper is likely to disrupt interdigitation due to the introduction of the extra carbon–carbon bond in the main chain. Additionally, if the aspartate residue is important for forming salt bridges or similar interactions, the isomerization will likely distance the aspartyl side chain and break these bonds. The disruption of a salt bridge by Asp-109 isomerization in αB crystallin has recently been probed by molecular dynamics and suggests that the loss of this interaction destabilizes the protein and leads to insolubility (55). These points may help explain decreased aggregation of certain peptides *in vitro*, which we have shown to form amyloid. If the aspartate is removed from steric zipper–forming regions, it may have no effect or provide needed flexibility to form a second steric zipper interface, enhancing aggregation.

In light of these results and in the context of the aging lens, we suggest that L-isoAsp–containing proteins and peptides take a number of different pathways toward becoming associated with WS and WI aggregates. We believe it is unlikely that the L-isoAsp residues are specifically targeted by proteases, as in our own data set, N- or C-terminal aspartate residues were rare, nor have aspartate residues been identified as a significant site of truncation by other literature studying the LMW lens fragments (44). Instead, to explain the high concentration of the L-isoAsp modification found in the WS aggregated lens protein fragments, we note that the native peptides themselves were highly prone to aggregation and insolubility, whereas the isomerized αA$^{52-65}$ and αA$^{89-98}$ forms aggregated less. The diminished capacity for these L-isoAsp peptides to cause aggregation may represent a tendency for certain isomerized peptides to become associated with WS protein aggregates, whereas their native counterparts associate with WI protein aggregates. Conversely, our experiments with a WI-derived anti-chaperone peptide demonstrated more severe protein precipitation and anti-chaperone activity in the isomerized form, and this peptide could not be found in our mass spectrometric analyses of the WS-HMW aggregates (34). Thus, it may be that the peptides in which the L-isoAsp modification produces more aggregation-prone properties are more likely to be found in the WI aggregates, whereas the peptides in which the L-isoAsp modification lessens these characteristics are more likely to be associated with WS aggregates.

Our results do not rule out that intact crystallins could become associated with HMW aggregates and isomerize while aggregated. These modified, aggregated crystallins could then become cleaved while in the aggregate form, possibly in

attempts by lens proteases to clear the light-scattering aggregates, and the modified peptides would then only be detected as distinct fragments by denaturing SDS-PAGE. However, the formation of the L-isoAsp residue may be less favorable in an aggregate because L-isoAsp residues are less readily formed within rigid structures, such as that of a large aggregate. In these structures, the peptide bond nitrogen is not often posed to attack the side chain carbonyl group of the aspartate or asparaginyl residue (Fig. 1) (56). The flexibility of short peptides naturally allows the backbone to sample a number of conformations in which the backbone nitrogen approaches the L-Asp side chain close enough for nucleophilic attack.

Irrespective of the path that gives rise to L-isoAsp–containing peptides in HMW aggregates, our results show that L-isoAsp may either increase or decrease the aggregation propensity of peptides, depending on the sequence of the fragment, and both are likely to contribute to WI and WS aggregation. Thus, the initial production of short crystallin fragments may represent a significant risk for the stability of other intact crystallins, and regulation of protease activity within the aging lens may help attenuate the onset of cataract. The lens tissue also acts as an ideal model of aging due to the lack of cellular and protein turnover, and the results presented here may be representative of a number of age-related diseases, such as the polypeptide aggregates of β-amyloid and tau in Alzheimer's disease, in which protein modifications at different sites have variable effects on protein aggregation.

Experimental procedures

WS and WI lens extract preparation

We studied 10 pairs of unfixed eye lenses, collected within 3 days post-mortem from three eye banks (San Diego Eye Bank (San Diego, CA), Sightlife (Seattle, WA), and OneLegacy (Los Angeles, CA)). None of the lenses had known ocular diseases. Eyes were a kind gift from Dr. Joseph Demer and were obtained in conformity with legal requirements. Lenses were thawed on ice. Whole lenses were lysed in 300–500 μl of ice-cold 50 mM Tris-HCl, pH 7.9, 150 mM NaCl in a glass tube with a Teflon pestle rotating at 300 rpm for two periods of 30 s each. In some cases, lens samples first had the nucleus removed using a 6-mm trephine. The remaining peripheral material was pooled for the preparation of the cortical extract. Both nuclear and cortical regions were then lysed with the same procedure as whole-lens extract. Lysates were spun at $20,000 \times g$ for 20 min at 4 °C. The supernatant was removed as the water-soluble extract and stored at −80 °C.

Pellets were resuspended in 300 μl of 6 M urea in 50 mM Tris-HCl, pH 7.9, 150 mM NaCl and homogenized by hand in an Eppendorf 1.6-ml microcentrifuge tube with 80 strokes of a form-fitting plastic pestle and rotated for 30 min at 4 °C (Kimble Chase Kontes pellet pestle 7495150000). After centrifugation at $15,000 \times g$ for 15 min at 4 °C, the supernatant fraction was set aside, and the pellet was rehomogenized with 50 strokes and then spun at $15,000 \times g$ for 15 min at 4 °C. The pellet was then rehomogenized and recentrifuged one additional time. The three supernatants were then combined as the WI extract and stored at −80 °C. Protein concentrations were

quantified by a Lowry assay after protein precipitation with 10% TCA (57).

Determination of L-isoaspartate levels by the PCMT1 methanol vapor diffusion assay

PCMT1 was used as an analytical reagent to quantify L-isoAsp levels in the lens extract proteins. In a final volume of 100 μl, 12.5–25 μg of lens extract protein was incubated for 2 h at 37 °C with 5 μg of PCMT1 (purified as a His-tagged enzyme from *Escherichia coli* containing the expression plasmid 34852 available from Addgene as described by Patananan *et al.* (58) with a specific activity at 37 °C of 5,300 pmol of methyl esters formed on KASA(isoD)LAKY/min/mg of enzyme). Final concentrations in the reactions included 135 mM BisTris-HCl, pH 6.4, and 10 μM [³H]AdoMet (prepared by a 1600-fold isotopic dilution of a stock of 72 Ci/mmol [³H]AdoMet (Perkin-Elmer Life Sciences, NET155H00) with nonisotopically labeled AdoMet (*p*-toluenesulfonate salt; Sigma-Aldrich A2408)). The reaction was stopped by adding 10 μl of 2 M sodium hydroxide, and 100 μl of the 110-μl mixture was transferred to a 9 × 2.5-cm piece of folded thick filter paper (Bio-Rad; catalogue no. 1650962) wedged in the neck of a 20-ml scintillation vial above 5 ml of scintillation reagent (Safety Solve, Research Products International, catalogue no. 121000), tightly capped, and incubated at room temperature. After 2 h, the folded filter papers were removed, the caps were replaced, and the vials were counted three times for 5 min each in a Beckman LS6500 scintillation counter. Background radioactivity in a reaction containing no substrate was determined by incubating the recombinant human PCMT1, 135 mM BisTris-HCl buffer, and 10 μM [³H]AdoMet as described above and was subtracted from the value obtained in experimental samples. Samples were analyzed in duplicate or triplicate as indicated in the figure legends.

Buffered-urea control reactions were carried out by resuspending the KASA(isoD)LAKY peptide in 50 mM Tris-HCl, pH 7.9, 150 mM NaCl with or without 6 M urea. Buffer alone, 10 pmol of KASA(isoD)LAKY, or 100 pmol of KASA(isoD)LAKY reactions in volumes of 25 μl were mixed with PCMT1 and [³H]AdoMet in a final volume of 100 μl as described above.

L-isoAsp quantification in soluble *versus* aggregated ⁶⁶SDRDKFVIFLDVKHF⁸⁰ peptide was performed in the same reaction conditions as described above. Aggregated peptide was prepared by dissolving ⁶⁶SDRDKFVIFLDVKHF⁸⁰ at 1 mg/ml in 50 mM Tris-HCl, pH 7.6, 150 mM NaCl (TBS) and shaking continuously for 5 days. Aggregate solutions were stored at room temperature until analysis. Soluble peptide solutions were prepared by dissolving ⁶⁶SDRDKFVIFLDVKHF⁸⁰ peptide in TBS with 10% DMSO and filtering through Corning® Costar® Spin-X® centrifuge tube filters immediately prior to analysis (Millipore Sigma, catalogue no. CLS8161).

Determination of endogenous lens protein PCMT1 activity by the methanol vapor diffusion assay

In a final volume of 100 μl, 10 μg of lens extract protein was incubated for 2 h at 37 °C with final concentrations of 100 μM KASA(isoD)LAKY peptide, 125 mM BisTris-HCl, pH 6.4, and 10 μM [³H]AdoMet, as prepared above. The reaction was stopped by adding 10 μl of 2 M sodium hydroxide, and 100 μl of the 110-μl mixture was assayed for volatile radioactivity, as described above. Background radioactivity was determined in a control lacking the lens extract and was subtracted from the value obtained in samples containing the lens extracts. Samples were analyzed in duplicate or triplicate as indicated in the figure legends.

L-Isoasparate analysis in lens polypeptides by SDS-PAGE fluorography

Analyses were performed using the approach described by Patananan *et al.* (58). Briefly, 25-μg extracts were analyzed in a 30-μl reaction volume with final concentrations of 74 mM Bis-Tris-HCl, pH 6.4, 6 μg of recombinant human PCMT1, 0.3 μM S-adenosyl-L-[*methyl*-³H]methionine (PerkinElmer Life Sciences; 75–85 Ci/mmol, 0.55 Ci/mmol in 10 mM H$_2$SO$_4$/ethanol (9:1, v/v)) and incubated for 2 h at 37 °C. The reaction was stopped by adding 5 μl of SDS-PAGE loading buffer (250 mM Tris-HCl, pH 6.8, 10% (w/v) SDS, 50% (v/v) glycerol, 5% (v/v) β-mercaptoethanol, and 0.05% (w/v) bromphenol blue). Samples were heated at 100 °C for 3 min and separated on a 12% SDS-polyacrylamide gel prepared in BisTris-HCl, pH 6.4, and run at 140 V for 1 h. Gels were stained with Coomassie (0.1% (w/v) Brilliant Blue R-250, 10% (v/v) glacial acetic acid, and 50% (v/v) methanol) for 1 h and destained with 10% (v/v) acetic acid and 15% (v/v) methanol. For fluorography, gels were subsequently incubated with EN3HANCE (PerkinElmer Life Sciences, catalogue no. 6NE9701) for 1 h, incubated in water for 30 min, and dried before the gels were exposed to film (Denville Scientific, 8 × 10-inch Hyblot Cl) for 2–3 days at −80 °C.

Size-exclusion chromatography and fluorography of lens extract protein fractions

Size-exclusion chromatography was performed on an ÄKTA prime system. A Superose 6, 10/300 GL gel filtration column (GE Healthcare, 17-5172-01, column length 30 cm, column inner diameter 10 mm, 13-μm average particle size) was equilibrated with 50 mM Tris-HCl, pH 7.9, 150 mM NaCl. Approximately 1 mg of lens extract protein was loaded for each run. One-ml fractions were collected at a flow rate of 0.4 ml/min at room temperature.

Twenty-five μl was removed from fractions for subsequent L-isoaspartate quantification by the PCMT1 methanol vapor diffusion assay as described above. The remaining portion of the fraction was precipitated with 10% TCA overnight at 4 °C and pelleted at 20,800 × *g* for 10 min at 4 °C, and the supernatant was discarded. Pellets were resuspended in 100 μl of 100 mM Tris-HCl, pH 7.9, 150 mM NaCl, 6 M urea, 0.1% SDS. Thirty μl of the resuspended pellet was radiolabeled in a reaction volume of 60 μl with a final concentration of 80 mM BisTris-HCl, pH 6.4, 6 μg of recombinant human PCMT1, 0.3 μM S-adenosyl-L-[*methyl*-³H]methionine and incubated for 2 h at 37 °C as described above. The reaction was stopped with 15 μl of SDS-PAGE loading buffer. Samples were heated at 100 °C for 3 min and separated on a 4–20%, 10-well ExpressPlus PAGE gel (GenScript, catalogue no. M42010) at 140 V for 1 h. Staining, enhancing, and fluorography proceeded as described above.

Mass spectrometric identification of low-molecular weight peptides in WS-HMW gel filtration fraction

Lens samples were separated by size-exclusion chromatography. The HMW fraction was concentrated in a Savant Speed-Vac concentrator and resuspended in 200 μl of 50 mM Tris-HCl, pH 7.9, 150 mM NaCl, 6 M urea. DTT was added to a final concentration of 5 mM, and the solution was incubated at 56 °C for 30 min. Iodoacetamide was then added to a final concentration of 14 mM and incubated at room temperature for 30 min. An additional amount of DTT was added at a final concentration of 5 mM, and the sample was incubated for 15 min at room temperature in the dark. The sample was then applied to a Microcon YM-30 30,000 MW cutoff filter (Millipore, Burlington, MA), and filtrate was collected for analysis. Equal amounts of the two samples were injected into the mass spectrometer. LC-MS/MS analysis was performed on an EASY-nLC 1000 coupled to a Q Exactive mass spectrometer with nano-electrospray ionization source (Thermo Fisher Scientific). The peptides were separated on a 75-μm diameter $\times$ 25 cm C18 reversed phase column (Thermo Fisher Scientific) with a gradient from 5% solvent B (0.1% formic acid in acetonitrile), 95% solvent A (0.1% formic acid in water) to 40% solvent B for 30 min at a constant flow of 300 nl/min, followed by an increase to 80% B during 30−50 min. The mass spectrometer was operated in data-dependent acquisition mode with a top 10 MS/MS method. Orbitrap resolving power was set to 70,000 at m/z 200 for MS1 and 17,500 at m/z 200 for MS2. Peptide mass spectra were searched against a database of 10 highly abundant human lens proteins using Proteome Discoverer, version 2.2 (Thermo Fisher Scientific) for identification and label-free precursor ion quantification. Identification was performed with the Mascot search engine with no enzyme specificity. The mass tolerances were set to 10 ppm and 0.02 Da for precursor and fragment ions. Methionine oxidation and cysteine carbamidomethylation were considered as dynamic modifications. Fixed-value PSM validator was used with maximum δCn of 0.05. For label-free quantitation, feature detection and retention time alignment were performed. Quantification values were based on intensities at the apex of each chromatographic peak. Peptide abundance was calculated as a sum of abundances of individual peptide-spectral matches that pass a quality threshold, and protein abundance was calculated as the sum of peptide abundances. Because there were major differences observed in the total abundances of searched peptides between the two samples, no normalization was performed. Instead, we compared total ion counts of the two runs, and they indicated close to equal peptide loading amounts. The raw abundances were scaled such that the average between the two samples was 100 for better visualization purposes in comparing the two samples and noticing peptides that exist only in one sample.

Purification of recombinant αB crystallin

The pET20-αB crystallin plasmid in the *E. coli* BL21 strain was a kind gift from Dr. Wayne Hubbell at the UCLA Stein Eye Institute. Cells were grown at 37 °C to an A_{600} of 0.6. Isopropyl β-D-1-thiogalactopyranoside was added to a final concentration of 0.5 mM, and cell growth continued for 3 h at 37 °C. Cells were harvested at 5,000 $\times$ g for 15 min at 4 °C. Cell pellets were resuspended in 20 mM Tris-HCl, pH 8.5, 10% glycerol, 1 M NaCl with 1 mM phenylmethylsulfonyl fluoride, 5 mM β-mercaptoethanol, 25 units/ml benzonase, and a Pierce protease inhibitor tablet, EDTA-free (Thermo Fisher Scientific, A32965). Cells were lysed on an Emulsiflex with three passages at 15,000 p.s.i. The lysate was spun at 9700 $\times$ g for 50 min at 4 °C. Nucleic acids were precipitated from the supernatant by the addition of 0.1% final polyethyleneimine and incubation at room temperature for 15 min. The mixture was spin at 13,000 rpm for 50 min. The supernatant was removed and subsequently loaded onto a 5-ml GE Healthcare HisTrap HP (catalogue no. 17-5248-01) equilibrated with wash buffer (20 mM Tris-HCl, pH 7.5, 100 mM NaCl, 5% glycerol, 20 mM imidazole). Proteins were eluted with an isocratic gradient from 0 to 100% elution buffer (20 mM Tris-HCl, pH 8.5, 100 mM NaCl, 5% glycerol, 500 mM imidazole) over 60 min at 1 ml/min. All fractions containing αB crystallin were pooled and applied to a 5-ml GE Healthcare HiTrap Q HP anion-exchange column (GE29-0513-25) equilibrated with wash buffer (20 mM Tris-HCl, pH 7.5, 5% glycerol). Proteins were eluted with an isocratic gradient from 0 to 100% elution buffer (20 mM Tris-HCl, pH 8.5, 5% glycerol, 1 M NaCl) over 70 ml at 1 ml/min. All fractions containing the polypeptide corresponding to αB crystallin after SDS-PAGE were pooled and loaded onto a HiPrep 16/60 Sephacryl S-200 HR gel filtration column (GE Healthcare 17116601). Proteins were separated at 0.4 ml/min over 200 ml of wash buffer (20 mM Tris-HCl, pH 7.5, 100 mM NaCl). Fractions containing αB crystallin were pooled, glycerol was added to a final concentration of 5%, and the protein was concentrated in an Amicon Ultra-15 centrifugal filter unit (Millipore Sigma, UFC901008).

Thioflavin T binding and light-scattering conditions for peptide aggregation assays

Synthetic peptides of ^{66}SDRDKFVIFLDVKHF^{80} with either an L-Asp or L-isoAsp residue at the 76-position were obtained from GenScript and dissolved in water at a concentration of 100 μM. ThT (Sigma, T3516) was dissolved at a concentration of 100 μM in 100 mM Tris-HCl, pH 7.6, 300 mM NaCl (2X TBS) (Sigma, 94158). For a final volume of 200 μl in a 96-well plate (Fisher, flat bottom, clear, nonsterile, 12565501), 100 μl of peptide stock was mixed with 100 μl of the 100 μM ThT stock. Plates were continuously shaken at 60 rpm, and fluorescence readings were taken every 15 min (excitation of 450 nm and 482 nm emission) in a Varioskan plate reader.

Synthetic αA crystallin peptides, ^{52}LFRTVLDSGISEVR^{68} and ^{89}VQDDFVEIH^{98}, were obtained from GenScript. For assessment of self-aggregation by light scattering, both native and isomerized ^{52}LFRTVLDSGISEVR^{68} peptides were dissolved at a concentration of 3 mg/ml in 50 mM Tris-HCl, pH 7.5, 1% DMSO. Because of the highly insoluble nature of the native ^{89}VQDDFVEIH^{98} peptide, both of the native and isomerized ^{89}VQDDFVEIH^{98} peptides were first dissolved at 2.5 mg/ml in 3% ammonium hydroxide in water (final concentration of 1.58 M from a 28% stock of Fisher certified ACS Plus reagent) and diluted to 2 mg/ml in a final concentration of 50 mM Tris-HCl, pH 7.5. The final pH of this solution as tested by pH strip (BDH VWR Analytical, catalogue no. BDH35309.606, pH range

![ASBMB]

J. Biol. Chem. (2019) 294(32) 12203–12219 **12217**

0–14) was found to be between pH 9 and 10. Two wells of 100-μl volume were assayed for each peptide solution in a Varioskan plate reader at 340 nm. Plates were continuously shaken at 600 rpm, and readings were taken every 15 min.

Chaperone inhibition assays

Saccharomyces cerevisiae ADH (Sigma, A7011), 125–150 μg; αB crystallin, 40–50 μg; and peptides, 40–50 μg, were mixed in a final volume of 300 μl of reaction buffer (50 mM sodium phosphate, pH 7.0, 100 mM NaCl, and 10 mM o-phenanthroline). Denaturation was monitored by absorbance at 360 nm every 15 min with continuous shaking at 60 rpm in a Varioskan plate reader.

Transmission EM

Formvar/carbon grids (Ted Pella, catalogue no. 01754-F) were prepared with 3 μl of αA$^{66-80,isoAsp76}$ fiber stock solution for 3 min and washed with water, and then 2 μl of Ted Pella uranyl acetate alternative (Ted Pella, catalogue no. 19485) was applied for 2 min, rinsed with water, and air-dried. Images were collected on an FEI T12 instrument.

Protein precipitation gel assays of peptide and lens extract mixtures

The αA$^{52-65,isoAsp58}$ and αA$^{89-98,isoAsp91}$ peptides were incubated with 500 μg of 47-year-old lens WS protein extract for 14 h at 37 °C in a final volume of 120 μl of 50 mM Tris-HCl, pH 7.9. Reactions were then spun down for 10 min at 960 × g. The supernatant was removed, and the pellet was resuspended in 40 μl of 1× SDS-PAGE loading dye and separated by SDS-PAGE on a 4–20%, 10-well ExpressPlus polyacrylamide gel (GenScript, catalogue no. M42010) at 140 V for 1 h. Densitometry of lanes was performed in ImageJ (59).

References

1. Forrester, J. V., Dick, A. D., McMenamin, P. G., and Roberts, F. (2016) *The Eye: Basic Sciences in Practice*, 3rd Ed., p. 102, Elsevier, New York

2. Cvekl, A., and Ashery-Padan, R. (2014) The cellular and molecular mechanisms of vertebrate lens development. *Development* **141**, 4432–4447 CrossRef Medline

3. Bassnett, S., Shi, Y., and Vrensen, G. F. (2011) Biological glass: structural determinants of eye lens transparency. *Philos. Trans. R. Soc. Lond. B Biol. Sci.* **366**, 1250–1264 CrossRef Medline

4. Delaye, M., and Tardieu, A. (1983) Short-range order of crystallin proteins accounts for eye lens transparency. *Nature* **302**, 415–417 CrossRef Medline

5. MacCoss, M. J., McDonald, W. H., Saraf, A., Sadygov, R., Clark, J. M., Tasto, J. J., Gould, K. L., Wolters, D., Washburn, M., Weiss, A., Clark, J. I., and Yates, J. R., 3rd (2002) Shotgun identification of protein modifications from protein complexes and lens tissue. *Proc. Natl. Acad. Sci. U.S.A.* **99**, 7900–7905 CrossRef Medline

6. Lampi, K. J., Wilmarth, P. A., Murray, M. R., and David, L. L. (2014) Lens β-crystallins: the role of deamidation and related modifications in aging and cataract. *Prog. Biophys. Mol. Biol.* **115**, 21–31 CrossRef Medline

7. Wilmarth, P. A., Tanner, S., Dasari, S., Nagalla, S. R., Riviere, M. A., Bafna, V., Pevzner, P. A., and David, L. L. (2006) Age-related changes in human crystallins determined from comparative analysis of post-translational modifications in young and aged lens: does deamidation contribute to crystallin insolubility? *J. Proteome Res.* **5**, 2554–2566 CrossRef Medline

8. Hains, P. G., and Truscott, R. J. W. (2007) Post-translational modifications in the nuclear region of young, aged, and cataract human lenses. *J. Proteome Res.* **6**, 3935–3943 CrossRef Medline

9. Hains, P. G., and Truscott, R. J. W. (2010) Age-dependent deamidation of lifelong proteins in the human lens. *Invest. Ophthalmol. Vis. Sci.* **51**, 3107–3114 CrossRef Medline

10. Ray, N. J. (2015) Biophysical chemistry of the ageing eye lens. *Biophys. Rev.* **7**, 353–368 CrossRef Medline

11. Truscott, R. J. W., and Friedrich, M. G. (2016) The etiology of human age-related cataract. Proteins don't last forever. *Biochim. Biophys. Acta* **1860**, 192–198 CrossRef Medline

12. McFadden, P. N., and Clarke, S. (1987) Conversion of isoaspartyl peptides to normal peptides: implications for the cellular repair of damaged proteins. *Proc. Natl. Acad. Sci.* **84**, 2595–2599 CrossRef Medline

13. Clarke, S. (2003) Aging as war between chemical and biochemical processes: protein methylation and the recognition of age-damaged proteins for repair. *Ageing Res. Rev.* **2**, 263–285 CrossRef Medline

14. Ni, W., Dai, S., Karger, B. L., and Zhou, Z. S. (2010) Analysis of isoaspartic acid by selective proteolysis with Asp-N and electron transfer dissociation mass spectrometry. *Anal. Chem.* **82**, 7485–7491 CrossRef Medline

15. Liu, M., Cheetham, J., Cauchon, N., Ostovic, J., Ni, W., Ren, D., and Zhou, Z. S. (2012) Protein isoaspartate methyltransferase-mediated ^{18}O-labeling of isoaspartic acid for mass spectrometry analysis. *Anal. Chem.* **84**, 1056–1062 CrossRef Medline

16. McFadden, P. N., and Clarke, S. (1986) Protein carboxyl methyltransferase and methyl acceptor proteins in aging and cataractous tissue of the human eye lens. *Mech. Ageing Dev.* **34**, 91–105 CrossRef Medline

17. Chondrogianni, N., Petropoulos, I., Grimm, S., Georgila, K., Catalgol, B., Friguet, B., Grune, T., and Gonos, E. S. (2014) Protein damage, repair, and proteolysis. *Mol. Aspects Med.* **35**, 1–71 CrossRef Medline

18. Lowenson, J. D., and Clarke, S. (1992) Recognition of D-aspartyl residues in polypeptides by the erythrocyte L-isoaspartyl/D-aspartyl protein methyltransferase: implications for the repair hypothesis. *J. Biol. Chem.* **267**, 5985–5995 Medline

19. Fujii, N., Sakaue, H., Sasaki, H., and Fujii, N. (2012) A rapid, comprehensive liquid chromatography-mass spectrometry (LC-MS)-based survey of the Asp isomers in crystallins from human cataract lenses. *J. Biol. Chem.* **287**, 39992–40002 CrossRef Medline

20. Hooi, M. Y. S., Raftery, M. J., and Truscott, R. J. W. (2012) Racemization of two proteins over our lifespan: deamidation of asparagine 76 in γS crystallin is greater in cataract than in normal lenses across the age range. *Invest. Ophthalmol. Vis. Sci.* **53**, 3554–3561 CrossRef Medline

21. Hooi, M. Y., Raftery, M. J., and Truscott, R. J. (2013) Accelerated aging of Asp 58 in αA crystallin and human cataract formation. *Exp. Eye. Res.* **106**, 34–39 CrossRef Medline

22. Zhu, X. J., Zhang, K. K., He, W. W., Du, Y., Hooi, M., and Lu, Y. (2018) Racemization at the Asp 58 residue in αA-crystallin from the lens of high myopic cataract patients. *J. Cell. Mol. Med.* **22**, 1118–1126 Medline

23. Lyon, Y. A., Sabbah, G. M., and Julian, R. R. (2018) Differences in α-crystallin isomerization reveal the activity of protein isoaspartyl methyltransferase (PIMT) in the nucleus and cortex of human lenses. *Exp. Eye Res.* **171**, 131–141 CrossRef Medline

24. Takata T., Shimo-Oka, T., Kojima, M., Miki, K., and Fujii, N. (2006) Differential analysis of D-β-Asp-containing proteins found in normal and

ASBMB

infrared irradiated rabbit lens. *Biochem. Biophys. Res. Commun.* **344,** 263–271 CrossRef Medline

25. Takata, T., and Fujii, N. (2016) Isomerization of Asp residues plays an important role in αA-crystallin dissociation. *FEBS J.* **283,** 850–859 CrossRef Medline

26. Li, L. K., Roy, D., and Spector, A. (1986) Changes in lens protein in concentric fractions from individual normal human lenses. *Curr. Eye Res.* **5,** 127–135 CrossRef Medline

27. Harrington, V., Srivastava, O. P., and Kirk, M. (2007) Proteomic analysis of water insoluble proteins from normal and cataractous human lenses. *Mol. Vis.* **13,** 1680–1694 Medline

28. Truscott, R. J. W., Mizdrak, J., Friedrich, M. G., Hooi, M. Y., Lyons, B., Jamie, J. F., Davies, M. J., Wilmarth, P. A., and David, L. L. (2012) Is *S*-methylation in the human lens a result of non-enzymatic methylation by *S*-adenosylmethionine? *Exp. Eye Res.* **99,** 48–54 CrossRef Medline

29. Harding, J. J., and Crabbe, M. J. C. (1984) The lens: development, proteins, metabolism and cataract. In *The Eye*, Vol. 1B (Davson, H., ed) pp. 207–492, Academic Press, Inc., New York

30. Yvon, M., Chabanet, C., and Pélissier, J. P. (1989) Solubility of peptides in trichloroacetic acid (TCA) solutions: hypothesis on the precipitation mechanism. *Int. J. Pept. Protein Res.* **34,** 166–176 Medline

31. Voorter, C. E., de Haard-Hoekman, W. A., van den Oetelaar, P. J., Bloemendal, H., and de Jong, W. W. (1988) Spontaneous peptide bond cleavage in aging α-crystallin through a succinimide intermediate. *J. Biol. Chem.* **263,** 19020–19023 Medline

32. Laganowsky, A., Benesch, J. L. P., Landau, M., Ding, L., Sawaya, M. R., Cascio, D., Huang, Q., Robinson, C. V., Horwitz, J., and Eisenberg, D. (2010) Crystal structures of truncated α and αB crystallins reveal structural mechanisms of polydispersity important for eye lens function. *Protein Sci.* **19,** 1031–1043 CrossRef Medline

33. Horwitz, J. (1992) α-Crystallin can function as a molecular chaperone. *Proc. Natl. Acad. Sci. U.S.A.* **89,** 10449–10453 CrossRef Medline

34. Santhoshkumar, P., Raju, M., and Sharma, K. K. (2011) αA-Crystallin peptide SDRDKFVIFLDVKHF accumulating in aging lens impairs the function of α-crystallin and induces lens protein aggregation. *PLoS One* **6,** e19291 CrossRef Medline

35. Roy, D., and Spector, A. (1976) High molecular weight protein from human lenses. *Exp. Eye Res.* **22,** 273–279 CrossRef Medline

36. Srivastava, O. P. (1988) Age-related increase in concentration and aggregation of degraded polypeptides in human lenses. *Exp. Eye Res.* **47,** 525–543 CrossRef Medline

37. Santhoshkumar, P., Udupa, P., Murugesan, R., and Sharma, K. K. (2008) Significance of interactions of low molecular weight crystallin fragments in lens aging and cataract formation. *J. Biol. Chem.* **283,** 8477–8485 CrossRef Medline

38. Srivastava, O. P., Srivastava, K., and Silney, C. (1996) Levels of crystallin fragments and identification of their origin in water soluble high molecular weight (HMW) proteins of human lenses. *Curr. Eye Res.* **15,** 511–520 CrossRef Medline

39. Groenen, P. J., Merck, K. B., de Jong, W. W., and Bloemendal, H. (1994) Structure and modifications of the junior chaperone α-crystallin: from lens transparency to molecular pathology. *Eur. J. Biochem.* **225,** 1–19 CrossRef Medline

40. Van Kleef, S. M., Willems-Thijssen, W., and Hoenders, H. J. (1976) Intracellular degradation and deamidation of α-crystallin subunits. *Eur. J. Biochem.* **66,** 477–483 CrossRef Medline

41. Sharma, K. K., and Santhoshkumar, P. (2009) Lens aging: effects of the crystallins. *Biochim. Biophys. Acta* **1790,** 1095–1108 CrossRef Medline

42. Takemoto, L. J. (1995) Identification of the *in vivo* truncation sites at the C-terminal region of α-A crystallin from aged bovine and human lens. *Curr. Eye Res.* **14,** 837–841 CrossRef Medline

43. Srivastava, O. P., and Srivastava, K. (2003) Existence of deamidated αB-crystallin fragments in normal and cataractous human lenses. *Mol. Vis.* **9,** 110–118 Medline

44. Harrington, V., McCall, S., Huynh, S., Srivastava, K., and Srivastava, O. P. (2004) Crystallins in water soluble-high molecular weight protein fractions and water insoluble protein fractions in aging and cataractous human lenses. *Mol. Vis.* **10,** 476–489 Medline

45. Grey, A. C., and Schey, K. L. (2009) Age-related changes in the spatial distribution of human lens α-crystallin products by MALDI imaging mass spectrometry. *Invest. Ophthalmol. Vis. Sci.* **50,** 4319–4329 CrossRef Medline

46. Lampi, K. J., Kim, Y. H., Bächinger, H. P., Boswell, B. A., Lindner, R. A., Carver, J. A., Shearer, T. R., David L. L., and Kapfer, D. M. (2002) Decreased heat stability and increased chaperone requirement of modified human βB1-crystallins. *Mol. Vis.* **8,** 359–366 Medline

47. Wenk, M., Herbst, R., Hoeger, D., Kretschmar, M., Lubsen, N. H., and Jaenicke, R. (2000) γS-Crystallin of bovine and human eye lens: solution structure, stability and folding of the intact two-domain protein and its separate domains. *Biophys. Chem.* **86,** 95–108 CrossRef Medline

48. Ajaz, M. S., Ma, Z., Smith, D. L., and Smith, J. B. (1997) Size of human lens β-crystallin aggregates are distinguished by N-terminal truncation of βB1. *J. Biol. Chem.* **272,** 11250–11255 CrossRef Medline

49. Senthilkumar, R., Chaerkady, R., and Sharma, K. K. (2002) Identification and properties of anti-chaperone-like peptides derived from oxidized bovine lens βL-crystallins. *J. Biol. Chem.* **277,** 39136–39143 CrossRef Medline

50. Raju, M., Santhoshkumar, P., and Sharma, K. K. (2012) αA-Crystallin-derived mini-chaperone modulates stability and function of cataract causing αAG98R-crystallin. *PLoS One* **7,** e44077 CrossRef Medline

51. Fujii, N., Takata, T., Fujii, N., and Aki, K. (2016) Isomerization of aspartyl residues in crystallins and its influence upon cataract. *Biochim. Biophys. Acta* **1860,** 183–191 CrossRef Medline

52. Truscott, R. J. W. (2007) Eye lens proteins and cataracts. In *Protein Misfolding, Aggregation, and Conformational Diseases* (Uversky, V. N., and Fink, A. L., eds) Springer, Boston

53. Thompson, M. J., Sievers, S. A., Karanicolas, J., Ivanova, M. I., Baker, D., and Eisenberg, D. (2006) The 3D profile method for identifying fibril-forming segments of proteins. *Proc. Natl. Acad. Sci. U.S.A.* **103,** 4074–4078 CrossRef Medline

54. Reissner, K. J., and Aswad, D. W. (2003) Deamidation and isoaspartate formation in proteins: unwanted alterations or surreptitious signals? *Cell. Mol. Life Sci.* **60,** 1281–1295 CrossRef Medline

55. Lyon, Y. A., Collier, M. P., Riggs, D. L., Degiacomi, M. T., Benesch, J. L. P., and Julian, R. R. (2019) Structural and functional consequences of age-related isomerization in α-crystallins. *J. Biol. Chem.* **294,** 7546–7555 CrossRef Medline

56. Clarke, S. (1987) Propensity for spontaneous succinimide formation from aspartyl and asparaginyl residues in cellular proteins. *Int. J. Pept. Protein Res.* **30,** 808–821 Medline

57. Thorne, C. J. R. (1978) *Techniques in Protein and Enzyme Biochemistry*, pp. 2–18, Elsevier/North-Holland, Ames, IA

58. Patananan, A. N., Capri, J., Whitelegge, J. P., and Clarke, S. G. (2014) Non-repair pathways for minimizing protein isoaspartyl damage in the yeast *Saccharomyces cerevisiae. J. Biol. Chem.* **289,** 16936–16953 CrossRef Medline

59. Schneider, C. A., Rasband, W. S., and Eliceiri, K. W. (2012) NIH Image to ImageJ: 25 years of image analysis. *Nat. Methods* **9,** 671–675 CrossRef Medline